ELECTRODYNAMICS OF NEUTRON STARS

F. Curtis MICHEL[a], **Hui LI**[b]

[a]*Department of Space Physics and Astronomy, Rice University, Houston, TX 77251, USA*
[b]*Theoretical Astrophysics, T-6, MS B288, Los Alamos National Laboratory, Los Alamos, NM 87545, USA*

ELSEVIER

AMSTERDAM – LAUSANNE – NEW YORK – OXFORD – SHANNON – TOKYO

ELSEVIER

Physics Reports 318 (1999) 227–297

PHYSICS REPORTS

www.elsevier.com/locate/physrep

Electrodynamics of neutron stars

F. Curtis Michel[a,*], Hui Li[b]

[a]*Department of Space Physics and Astronomy, Rice University, Houston, TX 77251, USA,*
[b]*Theoretical Astrophysics, T-6, MS B288, Los Alamos National Laboratory, Los Alamos, NM 87545, USA*

Received December 1998; editor: M.P. Kamionkowski

Contents

* Corresponding author.
E-mail addresses: fcm@curt.rice.edu (F.C. Michel), hli@lanl.gov (H. Li)

PII: S0370-1573(99)00002-2

Abstract

Although the standard model for radio pulsars is a rotating magnetized neutron star and the vast majority (if not all) of pulsars are thought to have appreciable inclination angles between the spin and magnetization axes, most theoretical papers use simplified field models (e.g., aligned spin axis and magnetic dipole axis). Deutsch long ago gave exact (in vacuo) closed expressions for these inclined fields (modulo some typos and oversights), but these expressions were rather clumsy and required extensive hand processing to convert into ordinary functions of radius and angle for the electromagnetic fields. Moreover, these expressions were effectively written down by inspection (no details of the derivations given), which leaves the reader with little physical understanding of where the various electric and magnetic field components come from, particularly near the neutron star surface where many models assume the radio emission is generated. Finally, rather little analysis of what these fields implied was given beyond speculation that they could accelerate cosmic rays. As pulsar models become more sophisticated, it seems important that all researchers use a consistent set of underlying fields, which we hope to present here, as well as understand why these fields are present.

It is also interesting to know what happens to charged particles from the star that move in these fields. Close to the star, ambient particles tend to simply $\boldsymbol{E}\times\boldsymbol{B}$ drift around the star with the same rotational velocity as the star itself. But far from the star, charged particles are accelerated away in the wave zone, as was first pointed out by Ostriker and Gunn. We expand their calculations using more general fields and elucidate the particle's dynamics accordingly. Very efficient acceleration is observed even for particles starting at $> 10^3$ light-cylinder distances. We also stress the effects of a non-zero radial magnetic field. Electrons are accelerated to much higher energies than, say, protons (not to the same energy as when the two cross a fixed potential drop). We pay particular attention to particles accelerated along the spin axis (particles that might be involved in jet formation). An important limitation to the present work is the neglect of collective radiation reaction. Single particle radiation reaction (e.g., Compton scattering of the wave flux) is *not* an accurate estimate of the forces on a *plasma*. We are working on remedying this limitation.

PACS: 97.60.Jd; 97.60.Gb

1. A brief history of radio pulsars

The first radio pulsar (then simply "pulsars" before similar objects radiating in X-rays were found) was discovered in 1967 and published after some delay [3]. Although the list of known pulsars is now of the order of 700, the original discoveries are still being observed in detail because they are among the brightest. New discoveries usually require intensive computer processing to pull their signals from the noise, and it is correspondingly laborious to study their properties. In general, pulsars (we will not discuss the X-ray versions, which are thought to radiate by an entirely different mechanism) are bright at low frequencies (e.g., 400 MHz) and dim at high frequencies (e.g., 4000 MHz). The pulses typically consist of one or more "components" closely packed together and separated by a very much longer interval of weak to non-detectable emission. At present, the shortest interval between successive pulses is about 1.5×10^{-3} s and the longest is about 5 s. Electrons in the interstellar medium delay the lower frequency parts of the pulse relative to the higher frequencies, and removing this relative delay (i.e., effectively lining up the pulses) yields the "dispersion measure", which is simply the line-of-sight path-integrated electron density, which in turn yields a rough distance estimate. There seems to be little or no observable difference between the fastest and the slowest, which pretty much excludes two of the three usual astronomical suspects for causing periodicity: orbital motion or physical oscillation in size. The shortest periods are within a factor of about 2 (or less) of the fastest that a nucleon-degenerate collapsed star ("neutron" star) can rotate. If the power source is the rotational energy, then one expects and indeed finds that the periods of all pulsars are increasing.[1] The only (so far) plausible reason for a tiny (a solar mass within 10 km) dense flywheel to lose energy is if it is magnetized and is emitting magnetic dipole radiation. An elementary estimate then gives a magnetic field of about 10^{12} gauss (G) for the magnetization. The fastest ("millisecond") pulsars necessarily have much weaker fields of about 10^{9} G (if they had the stronger field, they would spin down too quickly to hang around to be observed still spinning that fast). A histogram of numbers versus magnetic field suggests a bimodal distribution clustered about these two values. Why there should be two distinct preferred magnetic field strengths is a lively topic of speculation. "Weak field pulsar" would arguably be a better term than "millisecond pulsar", but it is rare for astronomical terminology to overcome casual usage.

The term "neutron star" is similarly a bit of a misnomer since there are a number of compositional transitions expected with depth, but the usual theoretical estimates have neutrons outnumbering protons by about 8:1. The main reason is that if the nucleons are resisting gravity by degeneracy pressure, electrons at the same densities have *huge* Fermi temperatures, which drive electron capture by the protons (inverse beta decay) to remove electrons and favor neutrons. One expected source of neutron stars is in the collapse of the cores of massive stars (one supernova model) and indeed some young radio pulsars are found inside of some young supernova remnants. Pulsar ages are estimated from the observed slowing down, $\dot{P}$, and the usual rule of thumb, $\tau_{\rm age}\approx P/\dot{P}$, which for the specific case of magnetic dipole radiation is $\tau_{\rm age}=P/2\dot{P}$.

The discovery of a pulsar within the Crab Nebula, generally thought to be the remnant of a historical supernova in 1054 AD, qualitatively solved the mystery of why continuum optical

[1] Unless contaminated by external gravitational forces on the neutron star.

radiation from that nebula is highly polarized and what powers it; evidently a magnetized plasma flows from the pulsar (not simply large amplitude electromagnetic waves in vacuo) and accumulates within a conducing shell of ejecta (visible in line emission). This general deductive analysis by elimination of what pulsars are (rotating magnetized neutron stars) seems broadly consistent with such observations.

2. Our basic approach

The obvious question ("Why are they emitting radio waves?") has not yet been answered. A series of theoretical models have been forwarded, which have either been found to wrong or to be charitably described as "incomplete". A generic (and non-committal) model would pose that there are some sort of discharges within the pulsar magnetosphere. We are then seeing these discharges rotate in and out of view. A serious theoretical problem is that a bright *low* frequency source from a *tiny* object vastly exceeds the black body emissivity at any plausible "temperature" and the spectrum is exactly the inverse of a hot black body (falling with frequency instead of rising). The radiation must then be coherent to begin with and then it must pass through a highly transparent medium to avoid being thermalized. A simple model having these properties would be discharges that bunched particles of one sign. At long wavelengths, the bunch radiates intensely as a single (highly charged) particle and at short wavelengths one eventually gets incoherent radiation from the individual particles (weaker emission by a factor of N, the number of particles in the bunch). This behavior is qualitatively just the spectral signature seen. The next alternative is some sort of maser action excited by counter-streaming in the (putative) discharges. Although we are not without preferences [4], such details are far beyond the basics we hope to lay out here. Most phenomenological models start with the assumption that discharges exist, usually posited to be confined to the vicinity of the magnetic poles, where the B field is usually taken to be dipolar with the magnetic axis inclined to the rotation axis.[2]

Our approach here is to start at the opposite limit, namely assume by contradiction that the inclined rotator has no discharges, try to find such solutions, and hope to find a paradoxical inconsistency. We would then know where discharges are required and why. For example, in the case of perfect alignment (an attractive theoretical simplification) we already find quiescent solutions with no obvious requirement for discharges other than one-shot transient ones as the system relaxes to a more stable configuration. This finding suggests that inclination is not only required to produce the "light-house" rotation of the discharges (i.e., the pulses), but is essential for maintaining the activity to begin with.

Not everyone is happy with this situation, and a few theorists still try to get an aligned rotator to do something. But in 15 years, not a single researcher in the field has come forward and shown how an inactive solution might be transformed into an active one.

Although our subject of interest is astrophysical in nature, the application closely parallels some interesting paradoxes in laboratory physics. In classical mechanics, the motions of bodies is

[2] More complicated fields are an obvious possibility, but pulsars are so ubiquitous (birthrates $\approx$ supernova rates) that we cannot require much beyond the simplest topology.

essentially trivial until one comes to the rotational motions, which require much more care in understanding. In the same way, electromagnetism is fairly straightforward even when uniform motions are added, but when rotation is added, textbook treatments are either non-existent or sometimes muddled at best [5]. For example, is rotating the observer equivalent to rotating the system, as it is for uniform translation? (No!) Does anything happen if you rotate a bar magnet about its axis? If you rotate a conductor and suddenly stop it, will a current flow? If you magnetize an object, is it set into rotation? If you stand a conductor in a gravitational field, do the conduction electrons "settle" toward the bottom? Some of these questions may be familiar, some may seem exotic.

When radio pulsars were discovered in 1967, an intense observational and theoretical effort soon zeroed down on these astrophysical objects as being rotating neutron stars having huge magnetic fields [4,6]. We are therefore back to one of the above questions, what happens if you rotate a magnet? [7].

An essential first step to understanding neutron star electrodynamics is an understanding of how the (assumed) conducting interior adjusts to rotation through its own magnetic field. Although the rotating magnetized neutron star model for pulsars seems a stable paradigm, the theoretical situation has been one of ups and downs, with very plausible models having proven to be unphysical. Given that three decades have passed without a theoretical breakthrough, it seems likely that enough different things are happening in connection with the generation of (highly coherent) radio emission from pulsars that it is correspondingly unlikely that one can simply guess at what is happening. Accordingly, it seems implausible that we can understand how pulsars function without first gaining some elementary levels of understanding of what *should* be happening in their vicinity.

3. Gravitating and rotating conductors

For rotating magnetized neutron starts, the Lorentz forces (on an electron, say) are huge compared to the gravitational forces, which in turn are usually orders of magnitude larger than the centrifugal forces.[3] Nevertheless, these inertial forces are often dominant.

A star such as our Sun can be regarded as a fully ionized plasma and hence an excellent conductor. The simplest model for a conductor is the free electron model. If we apply this model to the Sun, it would predict that the free electrons would attempt to "fall" to the center of the Sun. Such motion would produce a radial charge-separation electric field that in steady state would have the value

$$E_r = -m_e g/|e| \quad \text{(wrong)} . \tag{1}$$

In other words, the Sun would become negatively charged to keep the electrons from falling inwards against gravity. In fact, this estimate has the wrong sign and is several orders of magnitude

[3] Even near the so-called light cylinder distance, where it is often erroneously assumed that particles would "have" to rotate at the speed of light were they not slung away by the centrifugal force.

too small! Both the ions (mainly protons) and the electrons are better approximated as being gases, and under thermal equilibrium the electrons move much faster than the ions. A better approximation would be to assume that the electrons are essentially unbound gravitationally, in which case the Sun needs a positive charge to retain them (or will become positively charged by their loss). The situation becomes more extreme when we examine electron-degenerate stars (white dwarfs) and nucleon-degenerate ones (neutron stars) where the large electron Fermi energies require even larger stellar charges to retain the electrons.

If we now examine rotating stellar objects, we run into some semantical ambiguity of how we would exert a torque on either gas. It is easier to return to the laboratory scale where we can directly rotate (say) a metal sphere. Now the torques are distributed among the ions by the lattice forces. But in the free electron model the electrons do not see the lattice forces, and therefore the lattice will try to rotate through the electrons. The resultant ion current will produce a time-dependent (growing) magnetic field, and the accompanying induction electric field will then oppose the lattice rotation and transfer some of the torque to the electrons. Once a new steady state rotation has been achieved, a weak magnetic field of order

$$\Omega \approx \omega_c = eB/m_e \tag{2}$$

is roughly sufficient to tie the electrons to the lattice.[4] For the fastest known pulsar ($\Omega \approx 4000$ rad/s), this field would be only about 2×10^{-4} G. Ohmic dissipation would eventually remove this field (and any need for it, since the particles are now all corotating).

The point here is to emphasize that self-gravitation and rotation make for some deviations from our classic views of "classical" bulk objects. Adding magnetic fields makes for even more profound changes.

3.1. Rotating spherical conductor in B field

We now consider the case of a rotating spherical conductor in B field. The simplest symmetry is for the rotation axis to parallel a uniform external magnetic field. Although we assume the sphere to be conducting, the usual boundary condition at the surface,

$$\Phi = \text{const.}\,, \tag{3}$$

is *incorrect*. If the potential on the surface were constant (as appropriate for stationary conductors), the electric field inside would be identically zero (the desired result for a stationary conductor). But the magnetic field inside a rotating conductor provides an unbalanced Lorentz force

$$\boldsymbol{F} = \pm e\boldsymbol{V} \times \boldsymbol{B}\,, \tag{4}$$

where

$$\boldsymbol{V} = \Omega \times \boldsymbol{r} \tag{5}$$

[4] To our knowledge this toy problem has not been worked out exactly.

is the rotational velocity.[5] The consequence of this force is to separate the charges axially. Such a charge separation will clearly lead to an electric field of some sort. This effect is well-known in plasma physics, where it is usually termed the MHD (MagnetoHydroDynamic) condition and written variously as

$$\boldsymbol{E} + \boldsymbol{V}\times\boldsymbol{B} = \boldsymbol{0} \tag{6}$$

or

$$\boldsymbol{V} = \frac{\boldsymbol{E}\times\boldsymbol{B}}{B^2}\ . \tag{7}$$

The latter is more general since it is always possible provided that $E < cB$, while the first is only possible if additionally $\boldsymbol{E}\cdot\boldsymbol{B} = 0$.

The appearance of this electric field is perplexing to some physicists given that there is no induction, which is exactly correct. The resultant electric fields are indeed curl free. The short answer is that the conduction charges need to see both a $\boldsymbol{B}$ and an $\boldsymbol{E}$ field such that the $\boldsymbol{E}\times\boldsymbol{B}$ particle drift exactly matches the rotation rate of the star (we are largely repeating arguments in [4, Section 4.2]). If this electric field were absent, the Lorentz force on the corotating charges would move all the electrons outward (for the choice $\boldsymbol{B}\cdot\Omega > 0$) and all the ions inward, which would immediately create an electric field. But one does not need to follow the time-dependent particle dynamics, and their consequences, one simply requires of the interior that it ends up with $\boldsymbol{E}\cdot\boldsymbol{B} = 0$, one MHD condition. If we hook a stationary wire between the pole and equator of this rotating sphere, current will flow; this is simply a (fat) Faraday disk. Some textbooks even finesse this point (e.g., [8]) by imagining that one can transform into a rotating frame where the sphere is stationary but now the wire is moving in the magnetic field and "cutting" lines of force.[6]

If the magnet were an insulator (which is entirely possible in the laboratory, since magnetization arises from electron spin and not from electron conduction) the Lorentz force would be zero to first order on the neutral constituents. In their frame of reference the atoms would see an electric field which would cause some finite polarization and the latter would produce some (much weaker) electric field to be seen in the stationary frame. In the case of pulsars, even this effect would probably produce interestingly strong electric fields, but we will follow convention and simply assume the neutron star to be conducting, as it is expected to be from other arguments.

Altogether then, the Lorentz forces do the "inducing", and the terminology comes from the "unipolar inductor": the battery-like action of a metal disk rotating in an external magnetic field when the rim is shorted to the center, as shown in Fig. 1. Actually, there is a deep irony here because this rotating disk was apparently first suggested [10] by Faraday (and sometimes called a "Faraday disk"), presumably as an example of Faraday's law of induction!

[5] We generally reserve upper case for bulk quantities and lower case for particle attributes, unless esthetically distracting (e.g., coordinates).

[6] A somewhat dangerous assumption given that the rotating frame is non-inertial [9].

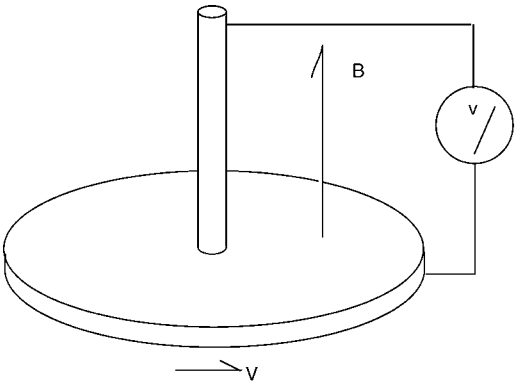

Fig. 1. Faraday disk, a rotating disk in a magnetic field develops a potential between the axis and the periphery, an elementary dynamo.

In the case of radio pulsars, the magnetic fields we will be interested in are estimated to be of the order of 10^{12} G. This estimate originally came from the assumption that the magnetic field is *orthogonal* and that the neutron star (an object nominally of about 1.4 solar masses and about 10 km radius) is slowing down owing to magnetic dipole radiation as if radiating into a vacuum [2]. The reader can simply regard such numbers as scaling estimates, quite apart from detailed justification. In any event the now-standard estimate – for all practical purposes *the definition* – is [11]

$$B = 3.2 \times 10^{19}(P\dot{P})^{\frac{1}{2}} \text{ G} \tag{8}$$

for the pulsar period P in seconds, with $\dot{P}$ being the dimensionless slowing down rate. Pulsars have periods in a wide range but mostly near one second, while the characteristic slowing down time is a few millions of years and hence a representative $\dot{P} \approx 10^{-15}$ giving a magnetic field of about 10^{12} G. Consequently, we will operate in a quite different parameter space from that of rotating magnets in the laboratory! Note also that the age of the galaxy itself is more like 10^{10} years, and therefore there must be a very large number of no-longer-seen pulsars.

4. Fields in the aligned case

First we discuss the vacuum electrodynamic fields expected about rotating magnetized stars and touch on some of the non-vacuum cases, where the neutron star is cloaked with (non neutral) plasma.

The model for the interior magnetic field is irrelevant to the (assumed dipolar) external field. A simple choice is to simply imagine that there is a point dipole at the center of the star. Alternatively, the interior field could be modeled as being uniform, although no one expects that *either* model would hold for an actual pulsar. Neither model should make any difference to what is happening in the exterior around the star, but certain points are easiest made in one or the other

picture. If a *central* dipole is aligned with the rotation axis, the fields are simply

$$B_r = 2B_0 \frac{a^3}{r^3} \cos\theta \quad \text{(all } r\text{)} , \tag{9}$$

$$B_\theta = B_0 \frac{a^3}{r^3} \sin\theta \quad \text{(all } r\text{)} , \tag{10}$$

where a is the stellar radius, and for positive B_0 the magnetic field points up out of the North ($\theta = 0$) pole, exactly opposite to the magnetic field of the Earth. Rotation of the conducting star through its own magnetic field (or perhaps less confusing, the rotation of each electron through the magnetic field created by all the other electrons) forms in essence a "fat" Faraday disk. Here, B_0 is the field strength at the equator, which is also that estimated[7] in Eq. (8).

4.1. The "*induced*" *electric quadrupole*

There are a number of ways of solving for the internal electric fields required to transform the corotational motion of the particles into $\boldsymbol{E} \times \boldsymbol{B}$ drift. One is the observation that in steady state the magnetic field lines must be equipotentials so that the electric field has no parallel component with which to drive currents (again, the so-called MHD condition in plasma physics). This condition can certainly be imposed on simple *models* if not necessarily on an active pulsar, where currents would be expected to circulate. Indeed, the simplest possibility works exactly, namely where the electrostatic potential inside is given by

$$\Phi = \Phi_0 \frac{a}{r} \sin^2\theta \quad \text{(inside star)} , \tag{11}$$

where

$$r = L \sin^2\theta \tag{12}$$

is an equation for dipole magnetic field lines, L being the equatorial (maximum) distance of the magnetic field line. Here the scaling requires (as we will establish)

$$\Phi_0 = B_0 a^2 \Omega . \tag{13}$$

Again, B_0 is the equatorial (dipole) magnetic field strength, exactly the quantity estimated in Eq. (8). Here positive Ω in Eq. (13) corresponds to counter-clockwise rotation as viewed looking down along the North pole, as is the case for the Earth's rotation. However, positive B_0 is opposite to that of the Earth but similar to that of Jupiter. These choices of sign (both positive or both negative) are a popular theoretical choice if it is assumed that radio emission comes from electrons accelerated over the magnetic polar caps. But this assumption gets us ahead of our discussion.

[7] Ironically, many theorists have labored for years under the impression that this estimate corresponded to the *polar* magnetic field strength!

It is direct to calculate that the resultant internal electric fields from the potential in Eq. (11)

$$E_r = \Phi_0 \frac{a}{r^2} \sin^2\theta \quad \text{(inside)} , \tag{14}$$

$$E_\theta = -2\Phi_0 \frac{a}{r^2} \sin\theta \cos\theta \quad \text{(inside)} , \tag{15}$$

which from Eq. (9) and (10) give $\boldsymbol{E}\cdot\boldsymbol{B} = 0$. The interior fields therefore satisfy our requirement that they do not accelerate corotating particles.

4.2. Rigid corotation

As a final check, let us calculate the drift velocity $\boldsymbol{V}_{\mathrm{D}} \equiv \boldsymbol{E}\times\boldsymbol{B}/B^2$ inside the star. Only the azimuthal component is nonzero,

$$(\boldsymbol{E}\times\boldsymbol{B})_\phi = \Phi_0 B_0 \frac{a^4}{r^5} \sin\theta(1 + 3\cos^2\theta) , \tag{16}$$

and since

$$B^2 = B_0^2 \frac{a^6}{r^6}(4\cos^2\theta + \sin^2\theta) \tag{17}$$

we find

$$V_{\mathrm{D}} = \frac{\Phi_0 r}{B_0 a^2} \sin\theta = r\Omega \sin\theta \tag{18}$$

as required for rigid rotation. This exercise is useful for checking that a consistent definition of Φ_0 has been used (especially with at least one factor of 2 floating around, namely whether B_0 is the equatorial or polar magnetic field strength).

The difficulty with this solution, which corresponds to a global solution, is the finite extent of the star. The required charge density is

$$\rho = \varepsilon_0 \nabla\cdot\boldsymbol{E} = 2\Phi_0\varepsilon_0 \frac{a}{r^3}(1 - 3\cos^2\theta) , \tag{19}$$

and the angular distribution is recognized to be the Legendre polynomial $P_2(\cos\theta)$, characteristic of a quadrupole distribution. But while it is necessary to have this charge distribution, which would arise from charge separation inside the conducting star, the solution is not sufficient when the charge distribution is truncated at the stellar radius, a. The missing charge outside the star is still required to give $\boldsymbol{E}\cdot\boldsymbol{B} = 0$ inside the star and must be replaced with something else that does just that. But before resolving that point, we should make one additional point about the internal charge distribution.

4.3. The required central charge

A quadrupole charge distribution (Eq. (19)) has no net charge, but the $1/r$ dependence of Φ in Eq. (11) requires a monopole moment, in addition to the distributed quadrupole. The value of the

charge is simply given by integrating E_r in Eq. (14) over a sphere using Gauss's law which gives

$$Q = 8\pi\varepsilon_0\Phi_0 a/3 \ , \tag{20}$$

hence

$$\Phi_{\text{monopole}} = \frac{2}{3}\Phi_0\frac{a}{r} \ . \tag{21}$$

The existence of this central charge is without question, although it is often neglected even in some theoretical papers. But the above evaluation does not explain why this central charge is required.

This required central charge is more explicit if we turn to the alternative internal magnetization model: a uniform internal magnetic field ($B_z = 2B_0$). Now $\boldsymbol{E}\times\boldsymbol{B}$ corotational drift requires an axial electric field which points toward the axis and increases linearly with axial distance,

$$E_\rho = -2\Omega B_0\rho \quad \text{(inside)} \ , \tag{22}$$

corresponding to a uniform internal charge density

$$\rho = \varepsilon_0\nabla\cdot\boldsymbol{E} = -4\varepsilon_0\Omega B_0 \ , \tag{23}$$

which gives (again) the net charge within the volume of the star

$$Q_1 = -\frac{16\pi}{3}\varepsilon_0\Omega B_0 a^3 = -2Q \quad \text{(inside)} \ . \tag{24}$$

Now that the magnetic field changes from the uniform field inside to pure dipole outside, the associated electric field changes from Eq. (22) to Eq. (14).[8] Such a transition demands a "surface" charge which is

$$\sigma = \varepsilon_0(E_r^{\text{ext}} - E_r^{\text{int}}) = 3\varepsilon_0\Omega B_0 a\sin^2\theta = \varepsilon_0\Omega B_0 a[2 + (1 - 3\cos^2\theta)] \ . \tag{25}$$

Integrating this over the whole sphere, we get a required total charge for making the transition to be

$$Q_2 = 8\pi\varepsilon_0\Phi_0 a = 3Q \ . \tag{26}$$

Thus, this "surface" charge proportional to $\sin^2\theta$ can be understood in terms of the sum of a uniform positive charge (Eq. (26)) and the accompanying quadrupole distribution. These then cause the star to have an effective "central" charge which is $Q = Q_2 + Q_1$ and the "internal" quadrupole moment as if it simply had a point dipole at the center as indicated by Eq. (20) in the model where the magnetic dipole is shrunk to a point at the stellar center.

As a note of clarification, the "surface" charge given in Eq. (25) is different from the usual definition of surface charge since it is required by the transition of uniform to dipolar field

[8] Even though this expression is given as an inside field, it is the correct expression for the immediate outside electric field also since the electrostatic potential is directly proportional to the magnetic field line function for a rigidly rotating star.

configurations and cannot be altered. As discussed in the following sections, there will also be the *induced* surface charge whose motion is subject to the surface electric fields, which can (and will) fly off the star.

4.4. The total charge of the star

The important point here is that the net *internal* charge Q of the star is not a free parameter but is determined by the magnetic dipole field and the condition $\boldsymbol{E}\cdot\boldsymbol{B}=0$ inside the star. If the star is not charged initially, a neutralizing charge $-Q$ will consequently appears on the surface. This neutralizing surface charge is again subject to the surface electric fields, which, as we will show later, are so strong that no surface charges could be maintained. Then these surface charges will fly off the star. If one considers a whole system consisting of the star and its surrounding plasma, then the surrounding plasma must contain a net amount of charge $-Q$ to ensure charge neutrality. But nothing said that the star had to be initially neutral, so the net system charge is actually arbitrary. The casual assumption that the overall system charge be zero probably contributes to theorists sometimes neglecting the intrinsic internal stellar charge Q. We will discuss the effects of varying total charge on the distribution of plasmas surrounding a star in the following sections.

4.5. The required external quadrupole

So far we have the elements of a solution, but no complete solution if the quadrupolar charge distribution is truncated beyond $r>a$. For a magnet (sometimes called a "terrella" if in the form of a sphere) rotated in the laboratory, the rest of the solution is no mystery, it simply corresponds the above pieces: the central charge and the quadrupolar space charge inside the sphere plus a surface charge. The surface charge is itself required to be quadrupolar since it replaces the missing external quadrupole charge distribution plus an arbitrary uniform surface charge (e.g., add $-Q$ if zero total charge desired).

The requirement for this external quadrupolar charge distribution follows again from the condition $\boldsymbol{E}\cdot\boldsymbol{B}=0$ inside the star. Let's just go through the derivation in small steps. At the surface, we can reinterpret the distributed quadrupole as a vacuum internal quadrupole generated by the external distributed charge and a vacuum external quadrupole generated by the internal distributed charge. In other words (here we normalize $\Phi_0 a\equiv 1$ and $r=1$ is the surface)

$$\frac{\sin^2\theta}{r}=\frac{A}{r}+\frac{B}{r^3}(1-3\cos^2\theta)+Cr^2(1-3\cos^2\theta)\,, \tag{27}$$

where the A term is the central monopole, B is the quadrupole potential due to charge separation inside the star, and C is the vacuum quadrupole potential due to charges external to r (e.g., a surface charge). What we are trying to determine here is what happens if the third component is absent, but for the moment we will assume it to be there. The coefficients A, B, and C are determined by the condition that the above equation holds and that $\boldsymbol{E}\cdot\boldsymbol{B}=0$ on the surface (owing to the differing r-dependences, the fields of each are different). Then we have for the potential at the surface ($r=1$)

$$\sin^2\theta=A+B(1-3\cos^2\theta)+C(1-3\cos^2\theta) \tag{28}$$

or $A = 2/3$ and $B + C = 1/3$. Each electric field component has a different dependence on r, but must give the same electric field at $r = 1$, so we can determine the coefficients by differentiating the potential, Eq. (27) with respect to r and then setting $r = 1$:

$$-\sin^2\theta = -A - 3B(1 - 3\cos^2\theta) + 2C(1 - 3\cos^2\theta) \tag{29}$$

which again requires $A = 2/3$, but $3B - 2C = 1/3$, hence $B = 1/5$ and $C = 2/15$.

We are now prepared to give the resultant electric potential for the case that the external distributed charge is missing. For example, if the rotation were of a spherical magnet in the laboratory, the distributed charge outside of the surface would simply be replaced by a quadrupolar surface charge that gave the same $Cr^2(1 - 3\cos^2\theta)$ potential inside. Then at every point, $\boldsymbol{E}\cdot\boldsymbol{B} = 0$ inside the magnet.

If instead we go to the case of a neutron star with nominal 10^{12} G field, radius of 10 km, and a rotation rate of 6 rad/s, the induced electrostatic fields are of the order of 6×10^{12} V/m. Not only is this a huge field, but we can see that an electron would be accelerated to relativistic energies over a few microns. Consequently, it has become common to assume that the work function of the neutron star is effectively zero, whereas for laboratory parameters the work function of a rotating terrella is effectively infinite. A neutron star would then differ fundamentally from the Earth in that there is no "ground" available. The neutron star has just the net charge Q and no other charges can be stored on it to vary that number. And no surface charge can be maintained! How then can we have $\boldsymbol{E}\cdot\boldsymbol{B} = 0$ inside without a surface charge? Clearly we then need an external quadrupolar space charge around the star.

4.6. *Surface charge redistribution: the electrosphere*

One way to provide the external quadrupole is simply to imagine that the internal charge separation simply extends beyond the star and to infinity. Now instead of the surface charge (terrella solution) we simply have the quadrupole charge separation density *everywhere*, even where there is no conductor to supply it. Mathematically this solution is fine but not physically. If we imagine the neutron star to be spun up, with the surface charge appearing briefly on the surface before being torn off,[9] what would we expect? Again with our sign convention, positive ΩB_0 corresponds to negative particles over the poles and positive particles in the equatorial plane. The positive particles would then appear at the equator and would have no place to go beyond following, to first order, the magnetic field lines. Since these lines are tightly closed, the positive particles could depart no further than about half a radius away from the surface. The quadrupole charge changes sign at $\cos^2\theta = 1/3$ or $\sin^2\theta = 2/3$ and from the dipolar field line equation Eq. (12) we have $L = 3/2$. The negative particles also move on closed magnetic field lines (except from the exact poles) and we will now show that there is a trapping region right above the poles. It is easiest to locate the trapping zone in the case where we start with the surface charge on the star, even if this will not be the final state. Then the power law dependence on C in Eq. (27) above to r^{-3} gives the

[9] We will show that the electric fields act to pull surface charge off regardless of sign.

external field from the surface charge, and the potential is then

$$\Phi = \frac{2}{3r} + \frac{(1 - 3\cos^2\theta)}{3r^3} . \tag{30}$$

We then satisfy $\boldsymbol{E}\cdot\boldsymbol{B} = 0$ inside the star, but now there is a trapping region starting at $r = a\sqrt{3}$ above the pole (where $\partial\Phi/\partial r = 0$) and arching to the surface. This trapping region is created by the net charge that the neutron star has, which is positive and attracts the electrons back to the star. However, the electrons are accelerated off the star by the quadrupole field, so they simply move out until the quadrupole field dies off sufficiently with distance (much faster than the monopole, of course). Thus any negative charges that might be introduced into the polar regions, or any negative charges that might escape the surface charge, will simply be trapped. The natural expectation of single charged plasma trapping is that the plasma forms a *non-neutral plasma*, a topic of extensive research in the laboratory [12–14]. Determining the exact distribution of such plasma is, however, a somewhat difficult task. But filling only portions of the volume about the neutron star with charge suggests the generic name "electrosphere". Early pulsar theory obsessed with the quadrupolar electric field "driving the electrons away", and neglect of the central positive charge guaranteed that the trapping feature would be missed. In the same way, the equatorial plane is also a locus of $\boldsymbol{E}\cdot\boldsymbol{B} = 0$ and in this case positive particles would accumulate here (repulsion by the central charge driving them to the most distance points on their magnetic field lines). In general, non neutral plasmas collect initially at loci of $\boldsymbol{E}\cdot\boldsymbol{B} = 0$.

4.7. Earnshaw's theorem

A standard proof in electrostatics texts is that one cannot trap particles in a static electric field because in the space outside of point charge, we have

$$\nabla^2\Phi = 0 \tag{31}$$

and such a Φ cannot have a local maxima or minima. But this theorem is not very robust, given that it fails if the slightest assumption is changed, such as adding other forces or introducing time dependence. Thus an electron is trapped in a classical atom (centrifugal force), in a Penning trap (magnetic force), in a Paul trap (oscillating electric fields), and in an aligned rotating magnetized neutron star (huge magnetic fields). The electrostatic trapping is only along the magnetic field lines, but the magnetic field itself inhibits escape in the tangential directions.

4.8. The totally filled magnetosphere (TFM) solution

Historically, this complexity was entirely missed and it was originally proposed [15] that the quadrupolar charge density inside the star simply continued as such to "infinity". The putative source of the external space charge was again particles from the surface. Unfortunately the apparent advantages of this assumption outweighed the deficiencies, because then this external quadrupolar charge distribution would have to rigidly corotate with the star (that was the boundary condition to begin with) and therefore at a distance c/Ω a physically impossible region

would be encountered beyond which the plasma particles would have to rotate faster than the speed of light. This distance was interpreted as the transition to a centrifugally driven wind-zone, which is evident in terminology that labels this distance as being the "light-cylinder distance", "cylinder" referring to locus where centrifugal force would become arbitrarily large in relation to the spin axis. Since a wind would drain particles from the surroundings, mainly on magnetic field lines leading to the polar regions, it was additionally assumed that charges would have to be accelerated from the poles to replace those lost. Much of the subsequent work concentrated on how such a polar acceleration region might produce coherent radio emission (the radio luminosity of radio pulsars being far too large to be incoherent and yet be emitted from such small areas of a neutron star). This diversion of effort away from fundamentals helped the model persist, and even today a few workers still struggle to try to make it work [16–18]. The fact that the particles drained from the polar regions would all be electrons (so assumed because accelerated electrons radiate most easily), and therefore that charge conservation should be violated, was regarded as a technical detail to somehow be fixed in this otherwise promising model. To a newcomer, it might seem astonishing that – in models for an actual radio pulsar, which surely must be an arcing, discharging, electromagnetic monster – something as comparatively benign in effect as centrifugal forces were imagined to be the *dominant* ones!

4.9. Numerical solutions

The electrosphere would generically be a dome of (negative) charge over each magnetic pole and a torus of (positive) charge around the equatorial zone. If these zones were to be expanded as much as possible, one should asymptotically approximate the entirely filled magnetosphere solution. The dome and torus configuration has been shown in numerical simulations [7] and reproduced in Fig. 2, which shows the case in which the net charge in the electrosphere is zero (thus the total system charge is again Q). The simulation was intentionally unsophisticated, with the surface charge replaced by a series of charged rings on the surface, which were released one at a time and allowed to find an equilibrium position. As more rings are released, the surface charge has to be readjusted to keep $\boldsymbol{E}\cdot\boldsymbol{B}=0$ inside the star. But as more charge accumulates outside, the electrosphere itself starts to remove the need for a surface charge and ultimately the simulation terminates naturally when there is no more surface charge to be removed.

As we have been discussing here, it is fairly obvious that "starting" the star with a surface charge and then releasing it will result in the positive particles from the equatorial zone simply popping out a short distance and being trapped by the intense closed magnetic field lines there. If the electrons are approximated as following magnetic field lines, there is only one field line on which they could escape, but that point is moot because there is a trapping region for electrons directly above the polar caps, which they occupy to form the domes. The build-up of the dome and torus are shown in Fig. 3. The electrons are attracted by the positive intrinsic charge of the star but repelled by the rotationally induced quadrupole electric field, which would drive them off the surface to begin with. But the monopolar electric field component will always dominate at some finite distance, thus they cannot escape. And the positive particles, which are repelled from the star, are trapped on the tightly closed equatorial field lines. The plasma density is far too low ($\approx 10^{11}\,\mathrm{cm}^{-3}$ [4]) for interchange instabilities to grow. Escape seems only possible if the total

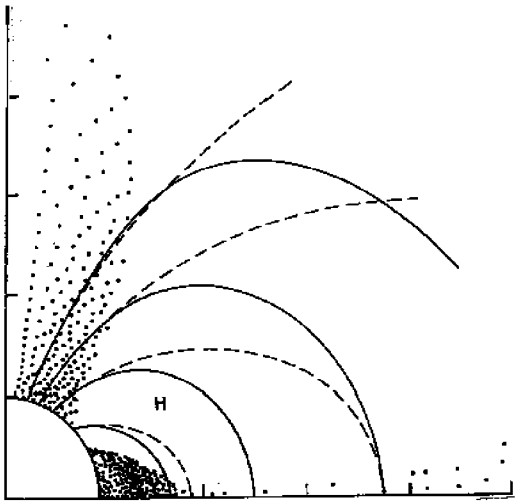

Fig. 2. Non neutral space charge distribution about an aligned rotator, as originally calculated [7].

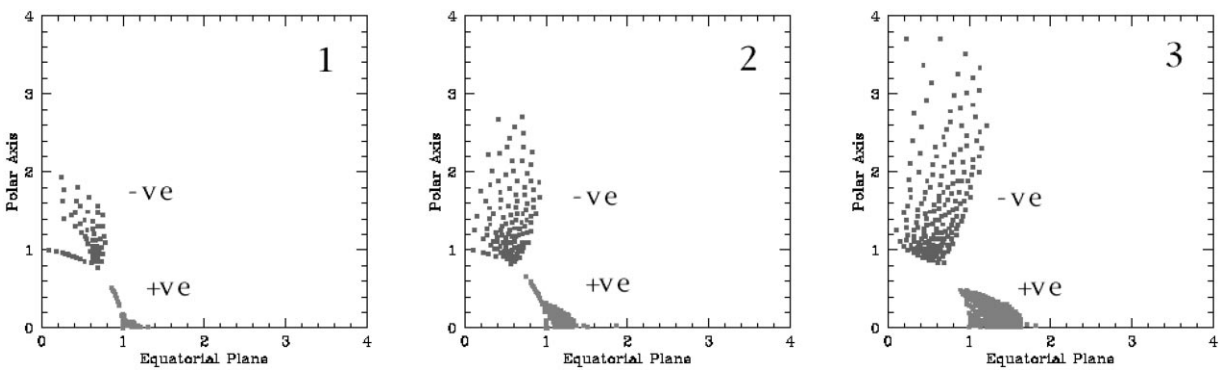

Fig. 3. Formation of the disk/torus electrosphere. The first figure is after one step, the second after 25 steps, and the final figure has terminated after 164 steps.

system charge is somehow driven to zero, which corresponds approximately to a configuration with all dome (extending to infinity) and virtually no torus.

4.10. Pair production

Even before the discovery of pulsars, it was realized [19] that gamma rays could convert into electron–positron pairs in strong magnetic fields. In active pulsars (as opposed to these idealized models) it is entirely possible that such pair production is essential in providing current carriers to power the activity. The important constraint has been that particles were assumed to be available only from the surface (positive particles would then be ions). If pair production effectively creates particles in vacuum regions (positive particles would then be positrons) the surface-origin

constraint is lifted. Such a source of ionization would surely modify the dome/torus configurations [20]. The process usually envisioned is energetic particles radiating curvature radiation to produce the gamma rays, which then convert to provide more energetic particles. In some models the successive particles are proportionately less energetic and in others an electric field maintains their energy. However, such a process is tightly localized to the vicinity of the neutron star because (1) it requires an intense magnetic field and the dipole fields weaken rapidly ($1/r^3$) with distance, and (2) because the surfaces of the dome and torus are $\boldsymbol{E}\cdot\boldsymbol{B}=0$ surfaces, so any accelerating electric field will vanish if the system tries to fill up and asymptotically approach the TFM solution. Consequently one expects modification of the dome/torus configuration, but it does not seem a plausible mechanism to drive activity in the aligned model [20].

Given that these non-neutral plasma distributions may be unfamiliar, it is probably worthwhile to go over Fig. 2 in some detail. First, notice that the dome and torus truncate abruptly as is evident even in this coarse discrete-particle simulation. These vacuum-to-plasma discontinuities are typical of non-neutral plasmas and contrast sharply with the tendency of quasi-neutral plasmas to fill all space by ambipolar diffusion along magnetic field lines. The charge density does not feather off smoothly to zero. Notice that the magnetic field lines (dashed) *cut across these surfaces*; it is not necessary that the field lines parallel the surfaces as is a possibility for stable density discontinuities in the quasi-neutral case. Next the decline in density of the dome is evident with increasing height. The charge distribution here is exactly that same as for the TFM (totally filled magnetopause) solution Eq. (19) but truncated at the discontinuities. The magnetic field lines have to be equipotentials where the plasma "shorts" them electrically to the surface, and the dome plasma must also rigidly corotate with the star. The equipotential lines are the solid ones and smoothly joint on to the magnetic field lines (dashed) inside the dome, as required, but outside they become more like spherical shells about the center of the star indicating the dominance of the central charge. The density should increase somewhat toward the axis, but our representation in terms of charged rings gives the opposite appearance, since the rings effectively represent wedges of charge density. The surrounding vacuum, which fills essentially all space is labeled "H" after a work by Holloway [21], wherein he pointed out that if one removed equatorial positive particles from the TFM solution on magnetic field lines leading to the (assumed negative) polar regions, there is no plausible way that they could be replaced and therefore a gap would have to form.[10] It turns out that some solutions are *all gap*! The torus is a bit more complicated and one can see what appears to be a dark band in the middle of it. What is happening here is that the magnetic field lines leading to the star only cut through part of the torus, and again here the charge density has to be the same as the TFM solution and the motion has to be corotation. But the outer parts are on magnetic field lines that pass through vacuum before reaching the surface and these are "open-circuited". Consequently, the plasma on the open-circuited magnetic field lines does *not* match that of the TFM solution, and the plasma here rotates somewhat faster than the star itself. Far from being a nuisance, this behavior is essential! If both the dome and torus had the same density as the TFM solution, then the internal quadrupole moment that they would generate would be *less* than that

[10] Holloway's argument is misunderstood in numerous recent publications: it would be invalid if any ionization process were present in the gap, but one can find Holloway cited as *justification* for gaps having just such action taking place.

given by the TFM solution and the latter provides exactly that required for $\boldsymbol{E}\cdot\boldsymbol{B}=0$ inside of the star. We have thrown effectively away both positive and negative particles from the TFM solution and the quadrupole moment must fall, unless there is an additional charge density added somewhere (here, the super-rotating part of the torus). Thus the system automatically finds a somewhat sophisticated solution.

On the other hand, the trapping has counter-intuitive properties. For example, a stray negative charge introduced near to the negative dome is "attracted" to the dome (actually it is attracted to the central positive charge more than it is repelled by the dome electrons). Ditto for positive particles above the torus. Moreover, these charged volumes cannot generally be neutralized. If a positive charge were introduced into the negative dome, it would see no macroscopic parallel electric field in first order, but in second order, the electrons have to be held up against gravity, so there will be a weak parallel electric field present to do this. But the very same field will accelerate the positive charge to the surface. Alternatively, the positive particle could have enough velocity to drift up out of the dome in which case it would be accelerated to the torus. The dome cannot be "neutralized".

4.11. Image charge

The way conductivity is handled here differs slightly from the standard textbook application in inertial systems. There the conductor is simply taken to be an equipotential ($\boldsymbol{E}=0$ inside). For our rotating systems, we have instead $\boldsymbol{E}\cdot\boldsymbol{B}=0$ inside. Given those conditions, in either system the introduction of a new test charge would produce image charges to appear on the surfaces of the conductors. But there is no discussion of image charges insofar as the charges in the dome and torus are concerned. The difference is in the assumption that charges can always leave the surface, so any invocation of image charges is therefore a temporary one, with the final state free of such charges. Thus the dome/torus configuration could, if one wished, be thought of having an image charge on the stellar surface (this would be a perfect quadrupole) in addition to which the star itself has the quadrupole surface charge needed to keep $\boldsymbol{E}\cdot\boldsymbol{B}=0$ inside. The two image charges are equal and opposite, corresponding to the resulting solution having no image charge. In electrostatics, there are no parallel space charge configurations owing to Earnshaw's theorem: they cannot be stable.

4.12. Boundary conditions

In numerical simulations, one actually has at least two limiting choices. One strategy is to keep the surface charge and release it (numerically) to form the electrosphere. But since the quadrupolar moment from the charges diminishes as they recede from the star, it is necessary to keep adding to the surface charge distribution as well, to keep $\boldsymbol{E}\cdot\boldsymbol{B}=0$ inside the magnet (star). Thus a number of release cycles are necessary to asymptotically approach an equilibrium solution.

The other choice, which is simpler in the aligned case, is just to discard the surface charge, and use the radial electric field as an indicator of how much surface charge there should have been and create the appropriate charges there (simulating currents flowing to the surface, not the creating of charge per se). Now one just continues, in either case, until no surface charge or no radial electric field is present, and one has driven $\boldsymbol{E}\cdot\boldsymbol{B}=0$ in the interior and by force balance $\boldsymbol{E}\cdot\boldsymbol{B}=0$ where ever there are charges.

The only difference is the *starting electric potential*, which is

$$\Phi_{SC} = \Phi_0\left(\frac{2}{3}\frac{a}{r} + \frac{1}{3}\frac{a^3}{r^3}(1 - 3\cos^2\theta)\right) \tag{32}$$

if the surface charge is present to begin with ($\boldsymbol{E}\cdot\boldsymbol{B} = 0$ inside the star), the external (vacuum) electric fields would be

$$E_r = \frac{2}{3}\Phi_0\frac{a}{r^2} + \Phi_0\frac{a^3}{r^4}(1 - 3\cos^2\theta) \quad \text{(outside)}\,, \tag{33}$$

$$E_\theta = -2\Phi_0\frac{a^3}{r^4}\sin\theta\cos\theta \quad \text{(outside)}\,. \tag{34}$$

These fields give $\boldsymbol{E}\cdot\boldsymbol{B} \neq 0$ at *just above* the surface (since we pass from $\boldsymbol{E}\cdot\boldsymbol{B} = 0$ inside through this surface charge), and we find again from Eq. (9) and Eq. (10), setting $r = a$, that

$$\boldsymbol{E}\cdot\boldsymbol{B} = \frac{4\Phi_0 B_0}{3a}\cos\theta(1 - 3\cos^2\theta) \quad \text{(surface)}\,, \tag{35}$$

showing (as advertised earlier) that the forces act to remove whichever sign of surface charge sitting on the surface.

Alternatively, we could instead assume the surface charge is missing in which case

$$\Phi_N = \Phi_0\left(\frac{2}{3}\frac{a}{r} + \frac{1}{5}\frac{a^3}{r^3}(1 - 3\cos^2\theta)\right), \tag{36}$$

but the star is "naked" and now does not have $\boldsymbol{E}\cdot\boldsymbol{B} = 0$ in the interior. The disadvantage here is that it is less clear where and in what order charges should be introduced, and since we can have full families of solutions depending on the overall system charge (the central charge plus whatever excess might reside in the electrosphere) one risks getting a slightly different equilibrium solution. In the case where we start with the surface charge, we can simply add a second uniform surface charge (which is invisible to the interior) and then start the process, which results in a unique family of solutions [22]. In Fig. 4 we show how the dome and torus vary as one changes the overall system charge. These configurations are each unique because the charges all start at the surface and follow magnetic field lines to their equilibrium positions. Unless one adds additional sources of ionization (most popularly, the pair-production cascades) or somehow allows particles to cross magnetic field lines, one will always get the same one-parameter family of configurations. In any case, once the electrosphere has been set up, the surface charge is gone and $\boldsymbol{E}\cdot\boldsymbol{B} = 0$ in the interior. For reasons special to the oblique rotator (to be discussed next), we shall prefer the choice in which the star initially has the required surface charge, which is subsequently released. As a final point, we show what happens when a totally filled magnetosphere is truncated at some finite distance. Since truncation removes space charge that is essential for $\boldsymbol{E}\cdot\boldsymbol{B} = 0$ in the interior, the resultant configuration is immediately rendered unstable and collapses into the dome and torus configuration, as shown in Fig. 5.

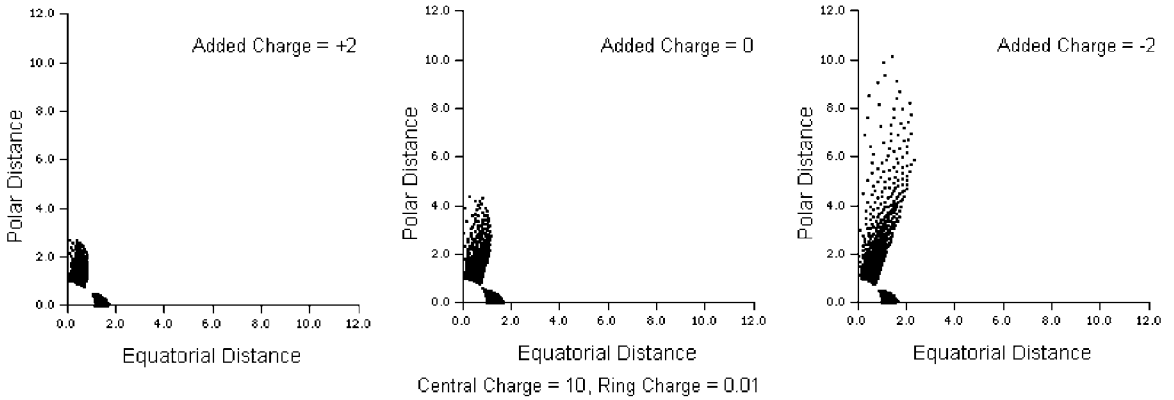

Fig. 4. Dome and torus for varying system charges. The central charge is taken to be + 15 units.

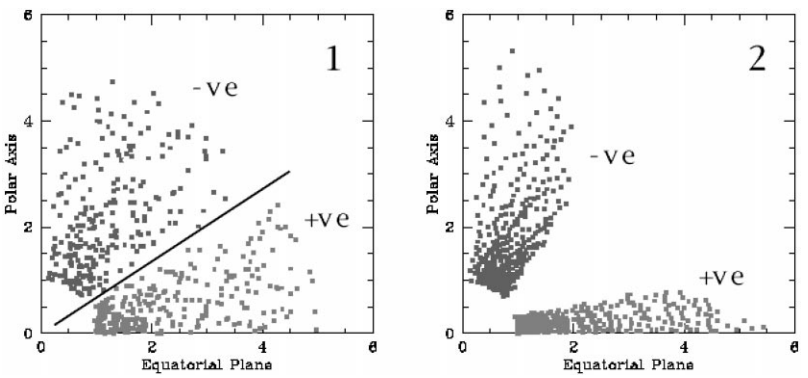

Fig. 5. Collapse of the totally filled magnetosphere when truncated. The line in the first figure is the zero charge density line separating minus from plus charges.

Even if we were to truncate the TFM at the "light cylinder", it would simply collapse to a stationary dome/torus configuration. Consequently, *the TFM is not a solution of the aligned model*!

4.13. Relevance to pulsars

From time to time the aligned model(s) have come under attack for the wrong reasons, namely that they would not pulse, owing to the axial symmetry. But pulsation has generally been assumed to be due to a finite angle between spin and dipole axis. The key assumption was that the physics would be "more or less the same", despite such misalignment. Now however, the assumption seems quite the opposite (at least in these quarters), namely that the physics will be significantly different! If an aligned rotator simply functions as an ion/electron trap on a huge scale, it is not too promising as a pulsar model. Curiously, a number of *idées fixes* are left over from the aligned model: (1) radio emission comes up out of the poles, (2) centrifugal forces are dominant, and (3) that it would even be active. The first consequence of dropping axial symmetry is that another important force is to be

found at the "light cylinder", namely the ponderomotive force of the large amplitude electromagnetic waves on the particles surrounding the pulsar. Indeed, energy radiated by such waves is where the magnetic field estimates (Eq. (8)) came from in the first place. However, if one *assumes* a wind, then the dipolar field lines would be forced open and the magnetic energy carried away by the wind gives exactly the same scaling. Thus, the energy density at the light cylinder scales as $B_{\rm lc}^2$, where $B_{\rm lc} = B_0 a^3/R_{\rm lc}^3$, with $R_{\rm lc} \equiv c/\Omega$, and the energy flux at c through the surrounding area $4\pi R_{\rm lc}^2$ scales as $B_0^2 a^6 \Omega^4$, exactly the same as for dipole radiation. Given the zeroth order defects in the aligned model insofar as pulsar function goes, we will examine the other limit of the inclined rotator, an orthogonal rotator.

5. The orthogonal rotator

Here we calculate the electric and magnetic fields near the star for the case that the dipole and spin axes are orthogonal.

Tilting the magnetic field (modeled as a central point dipole) through 90° gives the field components [4, Section 5.2],

$$B_r = 2B_0 \frac{a^3}{r^3} \sin\theta \cos(\phi - \Omega t) \quad (\text{all } r)\,, \tag{37}$$

$$B_\theta = -B_0 \frac{a^3}{r^3} \cos\theta \cos(\phi - \Omega t) \quad (\text{all } r)\,, \tag{38}$$

$$B_\phi = B_0 \frac{a^3}{r^3} \sin(\phi - \Omega t) \quad (\text{all } r)\,. \tag{39}$$

Now however the time dependence of the magnetic field directly induces electric fields as the next step of approximation ("true" induction if one wishes to make that distinction).

5.1. The induced electric quadrupole

These induction electric fields (*which are now only part of the total electric field*) are

$$E_r = 0, \quad (\text{induction fields only}) \ (\text{all } r)\,, \tag{40}$$

$$E_\theta = -\Phi_0 \frac{a}{r^2} \cos(\phi - \Omega t) \quad (\text{all } r)\,, \tag{41}$$

$$E_\phi = \Phi_0 \frac{a}{r^2} \cos\theta \sin(\phi - \Omega t) \quad (\text{all } r)\,. \tag{42}$$

These equations are not full solutions of Maxwell's equations but only the leading terms in the power series in $r\Omega/c$, which must terminate in the $1/r$ wave fields. Thus we implicitly assume $a\Omega/c \ll 1$ here, although it is not necessary to make this approximation, and further on we will give the full solutions, including the radiation fields, that would fill all of space if the space around

a rotating magnetized neutron star were a perfect vacuum (only possible if surface charge is retained, as we have seen).

Rather than derive the above components, we can simply check them, as for example starting with the ϕ-component

$$(\nabla \times \boldsymbol{E})_\phi = -\frac{\partial \boldsymbol{B}_\phi}{\partial t} \quad (\text{all } r) \tag{43}$$

we obtain from Eqs. (39) and (41)

$$\Phi_0 \frac{a}{r^3}\cos(\phi - \Omega t) = \Omega B_0 \frac{a^3}{r^3}\cos(\phi - \Omega t) \quad (\text{all } r) \tag{44}$$

so we require once again the boundary condition $\Phi_0 = \Omega a^2 B_0$. The remaining induction equations can easily be shown in directly the same way to be satisfied.

The time-dependence of these electric fields themselves give the displacement currents that provide the magnetic part of the outgoing wave fields, but we neglect that near the star.

Because we will no longer need to take into account the time-dependence of the fields, we will write $\phi - \Omega t \equiv \phi_s$ where ϕ_s is the longitude on the star, with $\phi_s = 0$ the longitude of the magnetic moment of the star.

We have not yet included the fact that the star is a conductor.

5.2. *Conducting star; a second "induced" electric quadrupole*

One can see that the star being a conductor is important by calculating for the interior (as well as exterior) fields that (Eqs. (38), (39), (41) and (42))

$$\boldsymbol{E}\cdot\boldsymbol{B} = B_0 \Phi_0 \frac{a^4}{r^5}\cos\theta \quad (\text{all } r)\,, \tag{45}$$

and therefore the induction electric field would drive currents in the star. Consequently, an internal quadrupole must appear to kill off this non-zero $\boldsymbol{E}\cdot\boldsymbol{B}$ below the surface. Again, this electric field appears spontaneously because it is "induced" by the non-zero Lorentz force that would be present otherwise. The required quadrupolar potential can be shown from direct calculation to be

$$\Phi = -\Phi_0 \frac{a}{r}\sin\theta\cos\theta\cos\phi_s \quad (\text{inside}) \tag{46}$$

which gives the additional electric fields

$$E_r = -\Phi_0 \frac{a}{r^2}\sin\theta\cos\theta\cos\phi_s \quad (\text{inside})\,, \tag{47}$$

$$E_\theta = -\Phi_0 \frac{a}{r^2}(\sin^2\theta - \cos^2\theta)\cos\phi_s \quad (\text{inside}), \tag{48}$$

$$E_\phi = -\Phi_0 \frac{a}{r^2}\cos\theta\sin\phi_s \quad (\text{inside})\,. \tag{49}$$

If we now calculate just the part of $\boldsymbol{E}\cdot\boldsymbol{B}$ contributed by these fields, we find

$$\boldsymbol{E}\cdot\boldsymbol{B} = -B_0\Phi_0\frac{a^4}{r^5}\cos\theta \quad \text{(inside)}\,. \tag{50}$$

Thus we see that the desired term canceling Eq. (45) has been obtained, and again the internal MHD condition will be satisfied.

Just as in the case of the aligned rotator, the internal quadrupole field requires a charge separation everywhere inside the star, while in fact the conducting star ends at the surface. In exactly the same way (except here there is no monopole component because this potential averages to zero), we conclude that we need an internal quadrupole (b) and an external quadrupole (c) such that

$$-\frac{\sin\theta\cos\theta\cos\phi_s}{r} = b\frac{\sin\theta\cos\theta\cos\phi_s}{r^3} + cr^2\sin\theta\cos\theta\cos\phi_s \quad \text{(inside)} \tag{51}$$

so immediately (at $r=1$) $b+c=-1$ and differentiating with respect to r

$$\frac{\sin\theta\cos\theta\cos\phi_s}{r^2} = -3b\frac{\sin\theta\cos\theta\cos\phi_s}{r^4} + 2cr\sin\theta\cos\theta\cos\phi_s \tag{52}$$

giving $-3b+2c=1$, and hence $b=-3/5$ and $c=-2/5$.

At this point we will examine just these leading near-field terms. Again from the point of view of numerical simulation, one has the choice of providing a surface charge to replace the missing space-charge beyond the star or simply leave the surface naked and tolerate a finite $\boldsymbol{E}\cdot\boldsymbol{B}$ inside the star until the electrosphere is set up. It proves to be somewhat less confusing to provide the surface charge because the external quadrupole field then cancels the induction field at the magnetic polar caps and thereby removes a nonzero component of $\boldsymbol{E}\cdot\boldsymbol{B}$ at the surface of the star that cannot actually pull particles from the star. Including such a term can make assessing where particles are removed on the basis of the surface value of $\boldsymbol{E}\cdot\boldsymbol{B}$ very confusing, but this is a technical point mainly of interest to someone doing numerical simulations.

If we keep the surface charge, then outside of the star we have a potential

$$\Phi_{SC} = -\Phi_0\frac{a^3}{r^3}\sin\theta\cos\theta\cos\phi_s \quad \text{(outside)} \tag{53}$$

which differs only in the power of r necessary for a vacuum solution external to the star. This difference alters the external electric fields to

$$E_r = -3\Phi_0\frac{a^3}{r^4}\sin\theta\cos\theta\cos\phi_s \quad \text{(outside)}\,, \tag{54}$$

$$E_\theta = -\Phi_0\frac{a^3}{r^4}(\sin^2\theta-\cos^2\theta)\cos\phi_s \quad \text{(outside)}\,, \tag{55}$$

$$E_\phi = -\Phi_0\frac{a^3}{r^4}\cos\theta\sin\phi_s \quad \text{(outside)}\,, \tag{56}$$

and when we add these to the induction electric fields (starting with Eq. (47)), we finally get

$$E_r = -3\Phi_0 \frac{a^3}{r^4} \sin\theta \cos\theta \cos\phi_s \quad \text{(outside)}\,, \tag{57}$$

$$E_\theta = \Phi_0 \left(\frac{a^3}{r^4} \cos 2\theta - \frac{a}{r^2} \right) \cos\phi_s \quad \text{(outside)}\,, \tag{58}$$

$$E_\phi = \Phi_0 \left(\frac{a}{r^2} - \frac{a^3}{r^4} \right) \cos\theta \sin\phi_s \quad \text{(outside)}\,. \tag{59}$$

If we now calculate the value of $\boldsymbol{E}\cdot\boldsymbol{B}$ *just above the surface* we get

$$\boldsymbol{E}\cdot\boldsymbol{B} = -\frac{4\Phi_0 B_0}{a} \sin^2\theta \cos\theta \cos^2\phi_s \quad \text{(outside)}\,. \tag{60}$$

Thus the action is to pull the surface charge off the surface and exactly matches where the surface charge is and what sign it has (just as we obtained in the aligned case). Surface charge, regardless of sign, is always pulled *off*. The charges appear at the surface in the first place because (by assumption) they cannot go any further. And there has to be a surface to terminate any rotating system lest material move faster than c.

The total electric field inside is then the sum of the induction field and the quadrupole field, hence

$$E_r = -\Phi_0 \frac{a}{r^2} \sin\theta \cos\theta \cos\phi_s \text{ (total int. field)} \quad \text{(inside)}\,, \tag{61}$$

$$E_\theta = -2\Phi_0 \frac{a}{r^2} \sin^2\theta \cos\phi_s \quad \text{(inside)}\,, \tag{62}$$

$$E_\phi = 0 \quad \text{(inside)}\,. \tag{63}$$

Notice that E_θ vanishes at $\theta = 0$ both inside and outside, as needed to eliminate a "surface" contribution to $\boldsymbol{E}\cdot\boldsymbol{B}$ from the induction electric field.

5.3. Rigid corotation

Let us now calculate $\boldsymbol{V}_D \equiv \boldsymbol{E}\times\boldsymbol{B}/B^2$ inside the star, for the special case of fields in the $\phi_s = 0$ plane (for reasons to become apparent)

$$(\boldsymbol{E}\times\boldsymbol{B})_\phi = \Phi_0 B_0 \frac{a^4}{r^5} \sin(1 + 3\sin^2\theta) \quad \text{(inside)} \tag{64}$$

while

$$B^2 = B_0^2 \frac{a^6}{r^6} (1 + 3\sin^2\theta) \quad \text{(inside)} \tag{65}$$

giving

$$V_{\rm D} = \frac{\Phi_0 r}{B_0 a^2} \sin\theta = r\Omega \sin\theta \quad \text{(inside)} \tag{66}$$

and again rigid corotation of charges with the star, as required.

In the orthogonal plane ($\cos\phi_{\rm s} = 0$), the electric field vanishes and the magnetic field is parallel to the corotational velocity vector. There is *no* corotational $\boldsymbol{E} \times \boldsymbol{B}$ drift. Here the charges corotate for the same reason that they would in an *unmagnetized* conducting sphere, not because the Lorentz force gives them a drift velocity but because they get in the way of their corotating neighbors. Corotation is *not* simply $\boldsymbol{E} \times \boldsymbol{B}$ drift in the orthogonal (or inclined) case.

5.4. Plasma distribution about the orthogonal rotator

The problem of numerically simulating the non-neutral plasma distribution about the orthogonal rotator have not yet been addressed. This problem lacks, of course, the symmetry that reduces a three-dimensional simulation to a two-dimensional one. Qualitatively it is clear that the quadrupolar surface charge will again leave the surface but not escape the system. Thus what was two domes and a torus for the aligned case now deform and the torus splits in two to give a total of 4 domes of alternating charge girding the star. For purposes of illustration, we can repeat the "GJ" treatment [15] by again assuming that the internal charge-separation density continues right through the surface to become a space-charge density and that the entire space becomes the "inside" solution. In the divergence of the (inside) electric field, only Eq. (62) contributes and we immediately get the (inside) charge-separation density [23,24]

$$\rho = -6\varepsilon_0 \Phi_0 \frac{a}{r^3} \sin\theta \cos\theta \cos\phi_{\rm s} \ . \tag{67}$$

If we simply extend this solution to everywhere outside the star á là GJ, we would definitely get an active system since the plasma would be driven out of the system by wave acceleration near the wave zone. Moreover, equal numbers of positive and negative charges could be driven away ("solving" the current closure problem). But at the same time, the polar cap charge densities and accelerating fields *vanish* at the polar caps. Note again that ρ is directly proportional to B_z:

$$\rho = -2\varepsilon_0 \Omega B_z \ . \tag{68}$$

Work is in progress to do these simulations for the orthogonal and also inclined rotator discussed below. Since pulsars must have (according to the conventional wisdom) inclined dipolar magnetic fields to even act as rotating "light-houses", the inclined case showing the transition between the two limits is of particular interest.

6. The inclined rotator

An inclined magnetic dipole is simply a linear superposition of the aligned and orthogonal limits. The only possible misstep here concerns $\boldsymbol{E} \cdot \boldsymbol{B} = 0$ inside the star because now we have two

components to each, $\boldsymbol{E} = \boldsymbol{E}_{\mathrm{A}} + \boldsymbol{E}_{\mathrm{O}}$ (Aligned and Orthogonal) and $\boldsymbol{B} = \boldsymbol{B}_{\mathrm{A}} + \boldsymbol{B}_{\mathrm{O}}$, so we need to confirm that the cross-terms $\boldsymbol{E}_{\mathrm{A}} \cdot \boldsymbol{B}_{\mathrm{O}} + \boldsymbol{E}_{\mathrm{O}} \cdot \boldsymbol{B}_{\mathrm{A}} = 0$ as well. Although the individual terms $\boldsymbol{E}_{\mathrm{A}} \cdot \boldsymbol{B}_{\mathrm{A}}$ and $\boldsymbol{E}_{\mathrm{O}} \cdot \boldsymbol{B}_{\mathrm{O}}$ vanish, the later condition is not guaranteed *in general*. However, it should hold because each pair is orthogonal and in the same ratio V_{D}. Thus for the orthogonal electric field components (Eq. (61)) and aligned magnetic field (Eq. (9)) we have

$$\boldsymbol{E}_{\mathrm{O}} \cdot \boldsymbol{B}_{\mathrm{A}} = -2\Phi_0 B_0 \frac{a^4}{r^5} \sin\theta \cos\phi_{\mathrm{s}} \tag{69}$$

while for the aligned electric field (Eq. (14)) and oblique magnetic field (Eq. (37)) we have

$$\boldsymbol{E}_{\mathrm{A}} \cdot \boldsymbol{B}_{\mathrm{O}} = 2\Phi_0 B_0 \frac{a^4}{r^5} \sin\theta \cos\phi_{\mathrm{s}} \tag{70}$$

and we see that indeed one can superimpose the two fields while retaining rigid corotation and zero field-aligned electric fields inside the star.

6.1. Summary of external near fields

Here we list the electric and magnetic fields *outside* the surface of a rotator inclined an angle ξ (see Fig. 6) with respect to the rotation axis and having a canceling surface charge that guarantees $\boldsymbol{E} \cdot \boldsymbol{B} = 0$ inside the star. Note that even though the interior satisfies the MHD condition, the exterior does not because one passes through the surface-charge layer. Thus if one creates and releases particles from the surface, the resultant internal quadrupole will violate the MHD condition and the surface-charge distribution will have to be reduced or modified. A simple numerical strategy would be to calculate, after having released a number of particles, their quadrupole moment inside the star and appropriately reduce that due to surface charges until

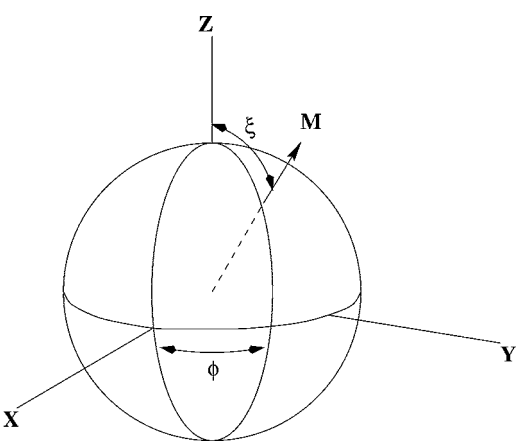

Fig. 6. Inclined rotator with magnetic moment directed along $\boldsymbol{M}$, rotating about the inertial axis z relative to axes x and y. The inclination angel ξ is fixed as ϕ changes. The usual polar angle θ is measured from z (not illustrated).

(to some finite accuracy) one cannot release another charge (each "charge" being a huge one compared to the electron charge, of course).

The magnetic fields are given from Eqs. (9) and (37),

$$B_r = 2B_0\frac{a^3}{r^3}(\cos\xi\cos\theta + \sin\xi\sin\theta\cos\phi_s)\,, \tag{71}$$

$$B_\theta = B_0\frac{a^3}{r^3}(\cos\xi\sin\theta - \sin\xi\cos\theta\cos\phi_s)\,, \tag{72}$$

$$B_\phi = B_0\frac{a^3}{r^3}\sin\xi\sin\phi_s\,. \tag{73}$$

The associated electric fields are then given from Eqs. (33) and (57)

$$E_r = \Omega a B_0\left(\frac{2}{3}\cos\xi\frac{a^2}{r^2} + \cos\xi\frac{a^4}{r^4}(1-3\cos^2\theta) - 3\sin\xi\frac{a^4}{r^4}\sin\theta\cos\theta\cos\phi_s\right), \tag{74}$$

$$E_\theta = \Omega a B_0\left[-2\cos\xi\frac{a^4}{r^4}\sin\theta\cos\theta + \sin\xi\left(\frac{a^4}{r^4}\cos 2\theta - \frac{a^2}{r^2}\right)\cos\phi_s\right], \tag{75}$$

$$E_\phi = \Omega a B_0\sin\xi\left(\frac{a^2}{r^2} - \frac{a^4}{r^4}\right)\cos\theta\sin\phi_s \tag{76}$$

6.2. Locus of trapping regions

In the case of $E \ll B$ (or at least $E_\perp \ll B$), it is well known that particles mainly experience acceleration along the $\boldsymbol{B}$ field ($\propto \boldsymbol{E}\cdot\boldsymbol{B}$) while the acceleration perpendicular to $\boldsymbol{B}$ *averages* to zero. Hence, $\boldsymbol{E}\cdot\boldsymbol{B} = 0$ defines the force-free surfaces. If we concentrate on the forces just above the surface of the star, the values of $\boldsymbol{E}\cdot\boldsymbol{B}$ simplify significantly and we get

$$\boldsymbol{E}\cdot\boldsymbol{B}\frac{3a}{4\Phi_0 B_0} = \cos^2\xi\cos\theta(1-3\cos^2\theta) + \sin\xi\cos\xi\sin\theta(6\sin^2\theta - 5)\cos\phi_s - 3\sin^2\xi\sin^2\theta\cos\theta\cos^2\phi_s\,. \tag{77}$$

If we wish to know the distribution in space above the surface, then we have (for $\phi_s = 0$)

$$M + N\frac{a^2}{r^2} = 0\,, \tag{78}$$

where

$$M = \tfrac{4}{3}\cos\xi(\cos\xi\cos\theta + \sin\xi\sin\theta) - \sin\xi(\cos\xi\sin\theta - \sin\xi\cos\theta)\,, \tag{79}$$

$$N = -4\cos^2\xi\cos^3\theta - \sin^2\xi\cos\theta(5 - 4\cos^2\theta) + \sin\xi\cos\xi\sin\theta(1 - 8\cos^2\theta)\,. \tag{80}$$

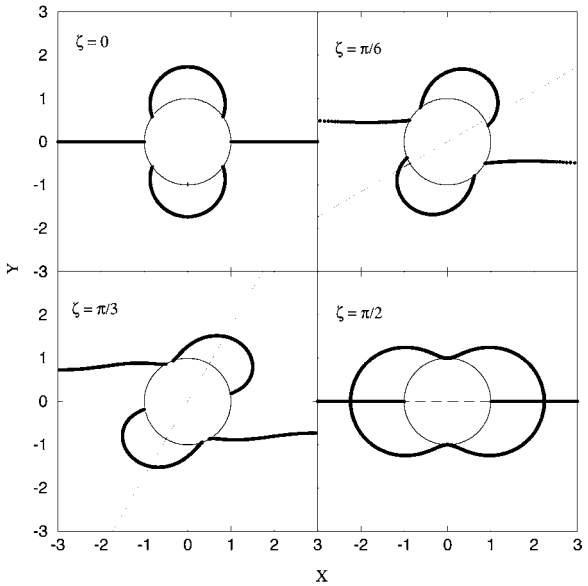

Fig. 7. Cross sections of force-free surfaces (thick solid lines) around a star (thin solid circle) using *vacuum* fields for various angles between spin and magnetic dipole axes (dashed line). An electric dipole from the central charge $\frac{2}{3}\cos\xi$ is also included. As more and more charges are "released" from the star surface, they will modify the fields around the star and "fill up" these force-free surfaces. Consequently, "domes" and "torus" will form instead.

The locus of $\boldsymbol{E}\cdot\boldsymbol{B}=0$ is shown in Fig. 7. Notice the difference between our results and those in Thielheim and Wolfsteller [25] where they omitted the central charge. Note that even in this most general case, the locus of zero charge density is the locus of zero B_z, since

$$\rho = -2\varepsilon_0\Omega B_z \tag{81}$$

once again.

6.3. Trapping regions

Notice in the aligned case that the trapping locus over the magnetic polar caps is a circle quite close to the surface. This trapping locus is what anchors the domes. In the equatorial plane, the plane is the trapping surface, and the positive particles would all accumulate here were it not for their self-repulsion so they form a torus instead [7].

7. The Deutsch fields

The full solution of the outside fields generated by a rotating magnetized sphere in vacuum with angle ξ between the spin and magnetic dipole axes (Fig. 6) has been given by Deutsch [1], with the (implicit) assumption that surface charges can somehow be maintained. Here, we give his original

solutions (in complex variables) for the sake of completeness (adopting changes in notations and correcting several typos)

$$
\begin{aligned}
B_r &= 2B_0\left\{\frac{a^3}{r^3}\cos\xi\cos\theta + \frac{h_1/\rho}{(h_1/\rho)_\alpha}\sin\xi\sin\theta\,\mathrm{e}^{\mathrm{i}\phi_\mathrm{s}}\right\},\\
B_\theta &= B_0\left\{\frac{a^3}{r^3}\cos\xi\sin\theta + \left[\left(\frac{\rho^2}{\rho h_2' + h_2}\right)_\alpha h_2 + \left(\frac{\rho}{h_1}\right)_\alpha\left(h_1' + \frac{h_1}{\rho}\right)\right]\sin\xi\cos\theta\,\mathrm{e}^{\mathrm{i}\phi_\mathrm{s}}\right\},\\
B_\phi &= B_0\left\{\left(\frac{\rho^2}{\rho h_2' + h_2}\right)_\alpha h_2\cos 2\theta + \left(\frac{\rho}{h_1}\right)_\alpha\left(h_1' + \frac{h_1}{\rho}\right)\right\}\mathrm{i}\sin\xi\,\mathrm{e}^{\mathrm{i}\phi_\mathrm{s}},
\end{aligned}
\tag{82}
$$

$$
\begin{aligned}
E_r &= E_0\left\{-\frac{1}{2}\frac{a^4}{r^4}\cos\xi(3\cos 2\theta + 1) + 3\left(\frac{\rho}{\rho h_2' + h_2}\right)_\alpha\frac{h_2}{\rho}\sin\xi\sin 2\theta\,\mathrm{e}^{\mathrm{i}\phi_\mathrm{s}}\right\},\\
E_\theta &= E_0\left\{-\frac{a^4}{r^4}\cos\xi\sin 2\theta + \left[\left(\frac{\rho}{\rho h_2' + h_2}\right)_\alpha\left(\frac{\rho h_2' + h_2}{\rho}\right)\cos 2\theta - \frac{h_1}{(h_1)_\alpha}\right]\sin\xi\,\mathrm{e}^{\mathrm{i}\phi_\mathrm{s}}\right\},\\
E_\phi &= E_0\left\{\left(\frac{\rho}{\rho h_2' + h_2}\right)_\alpha\left(\frac{\rho h_2' + h_2}{\rho}\right) - \frac{h_1}{(h_1)_\alpha}\right\}\mathrm{i}\sin\xi\cos\theta\,\mathrm{e}^{\mathrm{i}\phi_\mathrm{s}},
\end{aligned}
\tag{83}
$$

where $\rho = r\Omega/c$, $\alpha = a\Omega/c$, $\phi_\mathrm{s} = \phi - \Omega t$, and $E_0 \equiv \Omega a B_0$. h_1, h_2 and h_1', h_2' are spherical Bessel functions of the third kind with argument ρ and their derivatives, respectively. The subscript α means that the functions enclosed are evaluated at $\rho = \alpha$. Specifically, we have

$$
\begin{aligned}
h_1 &= \left[-\frac{1}{\rho} - \frac{\mathrm{i}}{\rho^2}\right]\mathrm{e}^{\mathrm{i}\rho},\\
h_1' &= \left[\frac{2}{\rho^2} + \mathrm{i}\left(\frac{2}{\rho^3} - \frac{1}{\rho}\right)\right]\mathrm{e}^{\mathrm{i}\rho},\\
h_2 &= \left[-\frac{3}{\rho^2} + \mathrm{i}\left(\frac{1}{\rho} - \frac{3}{\rho^3}\right)\right]\mathrm{e}^{\mathrm{i}\rho},\\
h_2' &= \left[\left(\frac{9}{\rho^3} - \frac{1}{\rho}\right) + \mathrm{i}\left(\frac{9}{\rho^4} - \frac{4}{\rho^2}\right)\right]\mathrm{e}^{\mathrm{i}\rho}.
\end{aligned}
\tag{84}
$$

It is apparent that the fields are a sum of the aligned component (terms with $\cos\xi$) and the orthogonal component (terms with $\sin\xi\,\mathrm{e}^{\mathrm{i}\phi_\mathrm{s}}$). Furthermore, orthogonal component radiates, thus all of them have a phase term $\mathrm{e}^{\mathrm{i}(\phi_\mathrm{s}+\rho-\alpha)}$ where the extra $\mathrm{e}^{\mathrm{i}(\rho-\alpha)}$ term comes from the spherical Bessel functions (e.g., terms such as $h_1/(h_1)_\alpha$). Hence, the fields ($\boldsymbol{F}$) can be written as[11]

$$
\boldsymbol{F} = \boldsymbol{F}(\text{aligned}) + \boldsymbol{F}(\text{dipole}) + \boldsymbol{F}(\text{quadrupole}),
\tag{85}
$$

[11] The analysis here is largely repeating Section 5.2 of Ref. [4], except for a few typos in Ref. [4]: Eq. (16d) should be multiplied by a factor of 2 and the multiplication factors (before and after Eq. (25)) differ for $\boldsymbol{B}$ and $\boldsymbol{E}$ by a factor of a (cf. our Eq. (88)).

where $\boldsymbol{F}$(aligned) is given as

$$B_r = 2B_0\frac{a^3}{r^3}\cos\xi\cos\theta\ ,$$

$$B_\theta = B_0\frac{a^3}{r^3}\cos\xi\sin\theta\ ,$$

$$B_\phi = 0\ ,$$

$$E_r = E_0\frac{a^4}{r^4}\cos\xi(1-3\cos^2\theta)\ ,$$

$$E_\theta = -E_0\frac{a^4}{r^4}\cos\xi\sin 2\theta\ ,$$

$$E_\phi = 0\ , \tag{86}$$

$\boldsymbol{F}$(dipole) is

$$B_r = 2B_0\frac{h_1/\rho}{(h_1/\rho)_\alpha}\sin\xi\sin\theta\,\mathrm{e}^{\mathrm{i}\phi_s}\ ,$$

$$B_\theta = B_0\left(\frac{\rho}{h_1}\right)_\alpha\left(h_1'+\frac{h_1}{\rho}\right)\sin\xi\cos\theta\,\mathrm{e}^{\mathrm{i}\phi_s}\ ,$$

$$B_\phi = \left(\frac{\rho}{h_1}\right)_\alpha\left(h_1'+\frac{h_1}{\rho}\right)\mathrm{i}\sin\xi\,\mathrm{e}^{\mathrm{i}\phi_s}\ ,$$

$$E_r = 0\ ,$$

$$E_\theta = -E_0\frac{h_1}{(h_1)_\alpha}\sin\xi\,\mathrm{e}^{\mathrm{i}\phi_s}\ ,$$

$$E_\phi = -E_0\frac{h_1}{(h_1)_\alpha}\mathrm{i}\sin\xi\cos\theta\,\mathrm{e}^{\mathrm{i}\phi_s} \tag{87}$$

and $\boldsymbol{F}$(quadrupole) is

$$B_r = 0\ ,$$

$$B_\theta = B_0\left(\frac{\rho^2}{\rho h_2'+h_2}\right)_\alpha h_2\sin\xi\cos\theta\,\mathrm{e}^{\mathrm{i}\phi_s}\ ,$$

$$B_\phi = B_0\left(\frac{\rho^2}{\rho h_2'+h_2}\right)_\alpha h_2\cos 2\theta\,\mathrm{i}\sin\xi\,\mathrm{e}^{\mathrm{i}\phi_s}\ ,$$

$$E_r = E_0 3\left(\frac{\rho}{\rho h_2' + h_2}\right)_\alpha \frac{h_2}{\rho}\sin\xi\sin 2\theta\, e^{i\phi_s}\,,$$

$$E_\theta = E_0\left(\frac{\rho}{\rho h_2' + h_2}\right)_\alpha \left(\frac{\rho h_2' + h_2}{\rho}\right)\cos 2\theta\sin\xi\, e^{i\phi_s}\,,$$

$$E_\phi = E_0\left(\frac{\rho}{\rho h_2' + h_2}\right)_\alpha \left(\frac{\rho h_2' + h_2}{\rho}\right) i\sin\xi\cos\theta\, e^{i\phi_s}\,. \tag{88}$$

Finally, adding the electrostatic monopole discussed above, we can recast Deutsch's solutions Eqs. (82) and (83) as, after taking real parts,[12]

$$B_r = 2B_0\frac{a^3}{r^3}\{\cos\xi\cos\theta + \sin\xi\sin\theta[d_1\cos\psi + d_2\sin\psi]\}\,,$$

$$B_\theta = B_0\frac{a^3}{r^3}\{\cos\xi\sin\theta - \sin\xi\cos\theta[(q_1 + d_3)\cos\psi + (q_2 + d_4)\sin\psi]\}\,,$$

$$B_\phi = B_0\frac{a^3}{r^3}\sin\xi\{-[q_2\cos 2\theta + d_4]\cos\psi + [q_1\cos 2\theta + d_3]\sin\psi\}\,, \tag{89}$$

$$E_r = E_0\frac{a^2}{r^2}\left\{\frac{2}{3}\cos\xi + \frac{a^2}{r^2}\cos\xi(1 - 3\cos^2\theta) - \frac{3}{\rho^2}\sin\xi\sin 2\theta[q_1\cos\psi + q_2\sin\psi]\right\},$$

$$E_\theta = E_0\frac{a^2}{r^2}\left\{-\frac{a^2}{r^2}\cos\xi\sin 2\theta + \sin\xi[(q_3\cos 2\theta - d_1)\cos\psi + (q_4\cos 2\theta - d_2)\sin\psi]\right\},$$

$$E_\phi = E_0\frac{a^2}{r^2}\sin\xi\cos\theta\{(q_4 - d_2)\cos\psi - (q_3 - d_1)\sin\psi\}\,, \tag{90}$$

where $\psi = \phi_s + \rho - \alpha$ (again, the extra term $\rho - \alpha$ comes from the Bessel functions) and

$$d_1 = \frac{\alpha\rho + 1}{\alpha^2 + 1}\,,$$

$$d_2 = \frac{\rho - \alpha}{\alpha^2 + 1}\,,$$

$$d_3 = \frac{1 + \alpha\rho - \rho^2}{\alpha^2 + 1}\,,$$

[12] A subroutine on solving these fields around a neutron star is available by sending an email to hli@lanl.gov.

$$d_4 = \frac{(\rho^2-1)\alpha+\rho}{\alpha^2+1},$$

$$q_1 = \frac{3\rho(6\alpha^3-\alpha^5)+(3-\rho^2)(6\alpha^2-3\alpha^4)}{\alpha^6-3\alpha^4+36},$$

$$q_2 = \frac{(3-\rho^2)(\alpha^5-6\alpha^3)+3\rho(6\alpha^2-3\alpha^4)}{\alpha^6-3\alpha^4+36},$$

$$q_3 = \frac{(\rho^3-6\rho)(\alpha^5-6\alpha^3)+(6-3\rho^2)(6\alpha^2-3\alpha^4)}{\rho^2(\alpha^6-3\alpha^4+36)},$$

$$q_4 = \frac{(6-3\rho^2)(\alpha^5-6\alpha^3)+(6\rho-\rho^3)(6\alpha^2-3\alpha^4)}{\rho^2(\alpha^6-3\alpha^4+36)}, \tag{91}$$

where all the d_i and q_i terms come from $\boldsymbol{F}$(dipole) and $\boldsymbol{F}$(quadrupole), respectively. For those who prefer Gaussian units over SI units, change E_0 to E_0/c in all the above equations.

We will now discuss these fields in near ($\rho \sim \alpha$) and far ($\rho\alpha \gg 1$) regions. First, in the near zone, the leading (considering the *comparative* importance) terms are

$$d_1 \approx 1, \qquad d_3 \approx 1, \qquad q_1 \approx \alpha^2/2, \qquad q_3 \approx (\alpha/\rho)^2,$$

which give (noting that $\psi \approx \phi_s$)

$$B_r = 2B_0\frac{a^3}{r^3}(\cos\xi\cos\theta + \sin\xi\sin\theta\cos\phi_s),$$

$$B_\theta = B_0\frac{a^3}{r^3}(\cos\xi\sin\theta - \sin\xi\cos\theta\cos\phi_s),$$

$$B_\phi = B_0\frac{a^3}{r^3}\sin\xi\sin\phi_s,$$

$$E_r = E_0\left(\frac{2}{3}\cos\xi\frac{a^2}{r^2} + \cos\xi\frac{a^4}{r^4}(1-3\cos^2\theta) - 3\sin\xi\frac{a^4}{r^4}\sin\theta\cos\theta\cos\phi_s\right),$$

$$E_\theta = E_0\left[-2\cos\xi\frac{a^4}{r^4}\sin\theta\cos\theta + \sin\xi\left(\frac{a^4}{r^4}\cos 2\theta - \frac{a^2}{r^2}\right)\cos\phi_s\right],$$

$$E_\phi = E_0\sin\xi\left(\frac{a^2}{r^2} - \frac{a^4}{r^4}\right)\cos\theta\sin\phi_s. \tag{92}$$

These are the same as Eq. (71)–(76), which show that the nearby $\boldsymbol{B}$ fields are dominated by the aligned component and *part* of the dipole component ($\propto 1/r^3$), whereas all components are present in $\boldsymbol{E}$ fields.

The asymptotic far fields ($\rho \gg 1$) can be obtained by noting that the only leading components are

$$d_2 \approx \rho, \qquad d_3 \approx -\rho^2 \tag{93}$$

which give us

$$B_r = 2B_0 \frac{a^3}{r^2} \frac{\Omega}{c} \sin\xi \sin\theta \sin\psi \,,$$

$$B_\theta = B_0 \frac{a^3}{r} \frac{\Omega^2}{c^2} \sin\xi \cos\theta \cos\psi \,,$$

$$B_\phi = -B_0 \frac{a^3}{r} \frac{\Omega^2}{c^2} \sin\xi \sin\psi \,,$$

$$E_r = E_0 \frac{a^2}{r^2} \frac{2}{3} \cos\xi \,,$$

$$E_\theta = -E_0 \frac{a^2}{r} \frac{\Omega}{c} \sin\xi \sin\psi \,,$$

$$E_\phi = -E_0 \frac{a^2}{r} \frac{\Omega}{c} \sin\xi \cos\theta \cos\psi \,. \tag{94}$$

Except for the electric monopole due to the central charge, these are the standard textbook wave fields.

Fig. 8 depicts some open field lines when ξ is nonzero. In Fig. 9, we show the deviation from static dipole magnetic field lines when the star is rotating by starting at the same footpoints on the star surface. Fig. 10 shows the role of electric dipole from the central charge. Fig. 11 compares the shape of the polar cap of a tilted rotating dipole with that of an aligned dipole. The polar cap is defined by the footpoints of those magnetic field lines whose maximum distance to the rotation axis is $R_{\rm lc}$. Fig. 12 shows the selected closed and open field lines of an orthogonal rotator and how they "cross" the light-cylinder distance. Fig. 13 shows the structure at large distances. In the plane perpendicular to the rotation axis and containing the rotating dipole, curiously, there are only *two* open field lines which are the Archimedes spirals. As we will show immediately below, these two spirals are nearly the minimum of $|B|$ at each r. The rest of field lines (with $\rho \gg 1$) all appear to converge to these two "null" lines. This behavior is rather counter-intuitive as one generally expects all open field lines in this plane spiral around to infinity. This derives from the consideration that the dominant B_r term falls as $1/r^2$ while B_ϕ drops as $1/r$, so the field line equation gives $dr/d\phi = \text{const.}$, which is a spiral. To show this explicitly, using Eq. (94) for an orthogonal $\xi = \pi/2$ rotator and in the plane of $\theta = \pi/2$, one actually finds

$$\rho B_r/B_\phi = -\frac{2\sin\psi}{\sin\psi} = -2 \tag{95}$$

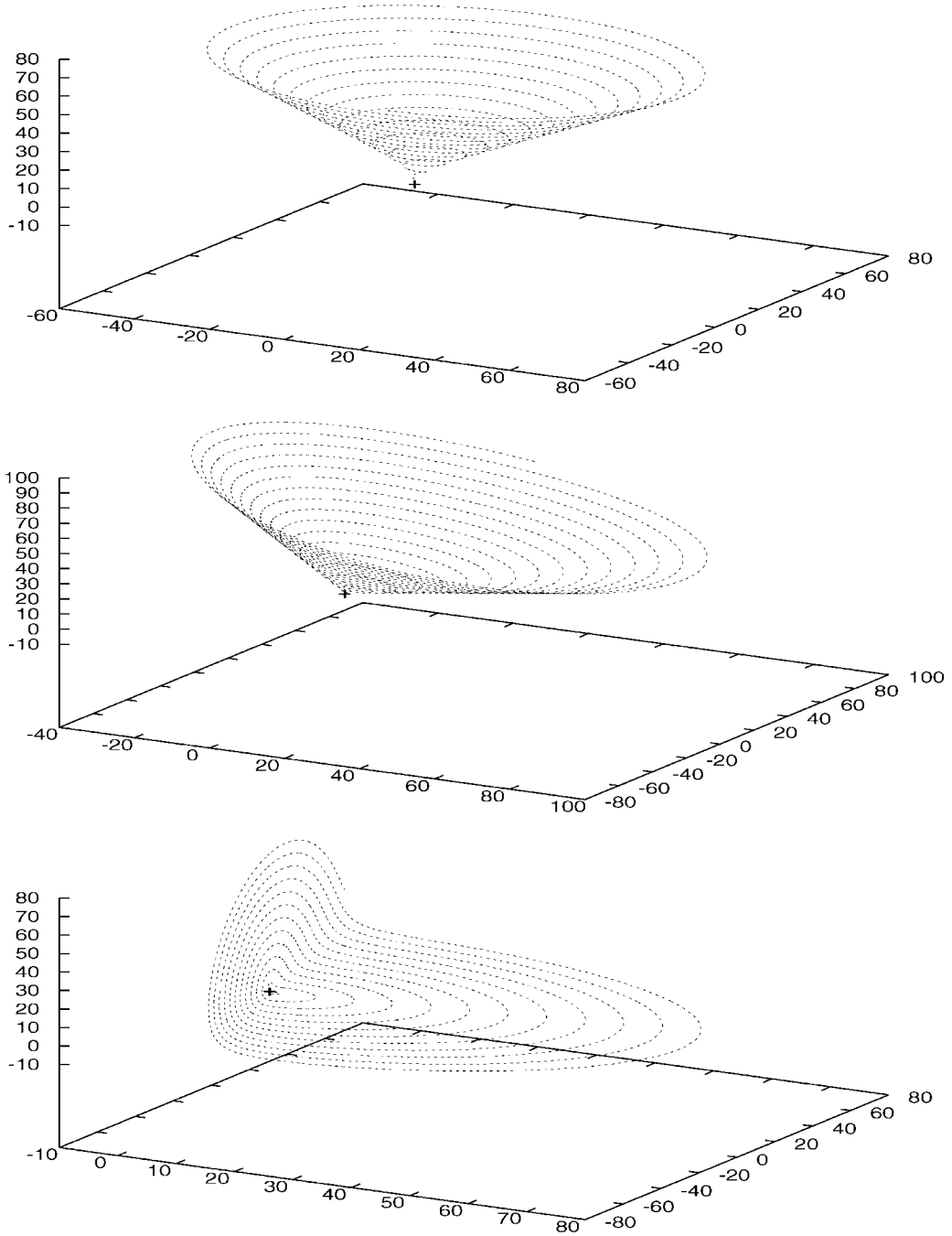

Fig. 8. Single polar field lines ($\theta = \xi$ and $\phi = 0$) for $\xi = 5°$, 45°, and 85° from top to bottom, respectively. These field lines (as well as their near neighbors) are presumably the "open" field lines that go out to infinity. The rotation axis is up and the magnetic axis is tilted to the right. All dimensions are in units of R_{lc} and parameters similar to Crab pulsar are used.

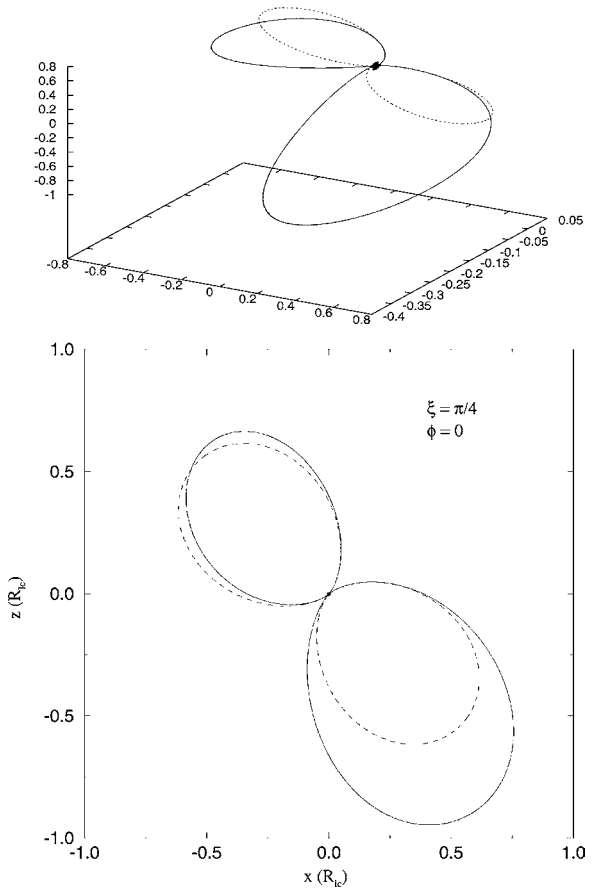

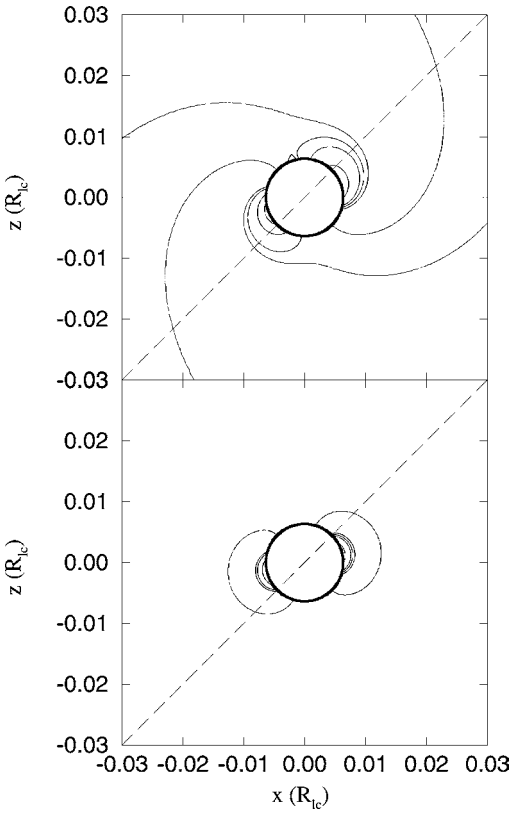

Fig. 9. 3-D and a side-view (2D) of two closed field lines (solid lines) starting with $\phi = 0$ and $\theta \approx \xi \pm (a/R_{\rm lc})^{1/2}$ from a titled rotator ($\xi = 45^\circ$). The dashed lines represent the case if the star is not rotating. The rotation axis is up and the magnetic axis is titled to the right. All dimensions are in units of $R_{\rm lc}$ and parameters similar to Crab pulsar are used.

Fig. 10. The electric field lines near the star with (upper panel) and without the central charge (lower panel). Here, $\xi = 45^\circ$, $\phi = 0$ and two panels have the *same* set of initial θ angles. It is clear that the radial component from the electric dipole "pushes" the field lines out. The rotation axis is up and the magnetic axis is titled to the right (dashed line). All dimensions are in units of $R_{\rm lc}$ and parameters similar to Crab pulsar are used.

which implies that

$$|\Delta\rho| = |\Delta r/R_{\rm lc}| = 2\Delta\phi\ . \tag{96}$$

In other words, the distance between the same field line is 4π instead of 2π as expected for one wavelength. Hence the casual expectation that all open field lines spiral around is not right. To do this correctly, one has to realize that the "correction" terms in $\boldsymbol{B}$ become important when $\sin\psi \to 0$.

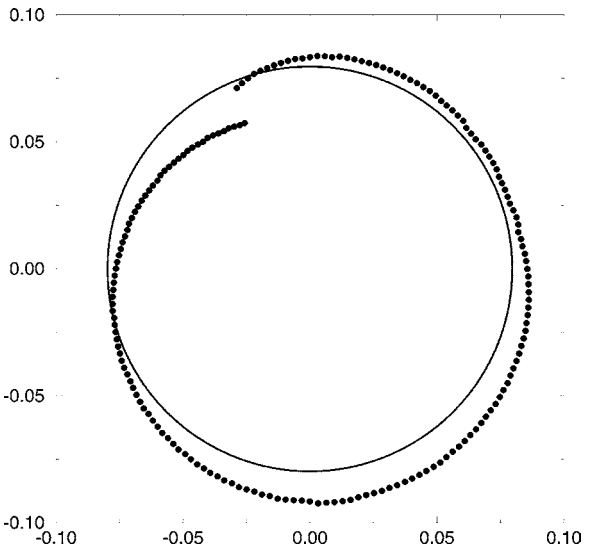

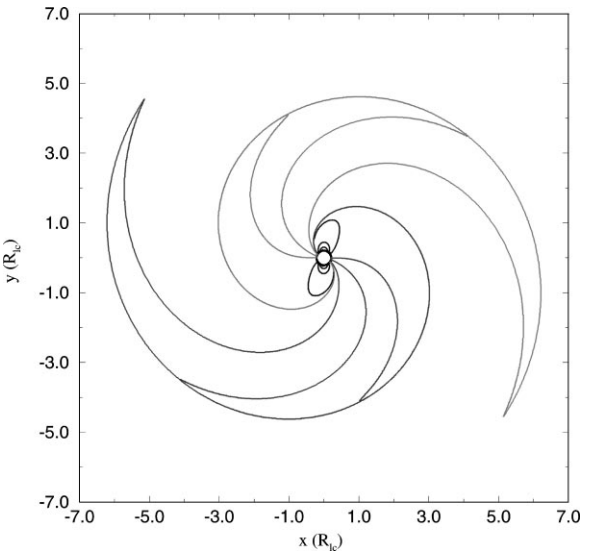

Fig. 11. The shape of the polar cap for $\xi = 45°$. The magnetic axis is at $(0,0)$ and pointing out of the paper, and the rotation axis is tilted to the left. Filled dots indicate the footpoints of the field lines with the maximum distance to the rotation axis being $R_{\rm lc}$. Solid line represents an aligned dipole case. Parameters similar to Crab pulsar are used.

Fig. 12. Selected closed and open field lines for an orthogonal rotator. All field lines are in the plane perpendicular to the rotation axis and containing the rotating dipole. (The dipole axis is pointing to the right.) As the distance from the star increases, the radial component of the open field lines decreases, so that they all appear to converge to two "null" field lines, which are the locus of (nearly) minimum B. The null field lines form two Archimedes spirals, separated by π, and going out to infinity (not shown here). Note that the radial component of the open field lines should never be exactly zero. All dimensions are in units of $R_{\rm lc}$ and a period of 1 ms is assumed in order to resolve the size of the star.

Using the full expressions from Eq. (89), we need the following ratio

$$\frac{\rho B_r}{B_\phi} = -\frac{2(\alpha\cos\psi + \sin\psi)}{(\alpha + 1/\rho)\cos\psi + \sin\psi} \tag{97}$$

to be -1 for an outgoing spiral. Hence, we find that the Archimedes spirals are only possible for specific ψ,

$$\psi = \arctan(-\alpha + 1/\rho) \quad \text{or} \quad \pi + \arctan(-\alpha + 1/\rho)\,. \tag{98}$$

These are the two spirals seen in Fig. 13. Note that with these ψ, B_r and B_ϕ are nearly zero, thus the spirals are indeed almost the minimum of $|B|$ at that distance r.

8. The particle motions

Having discussed the sort of fields that we would expect about an oblique rotator *in vacuo*, we will examine some of the particle dynamics in such fields. Particle acceleration (and radiation) in

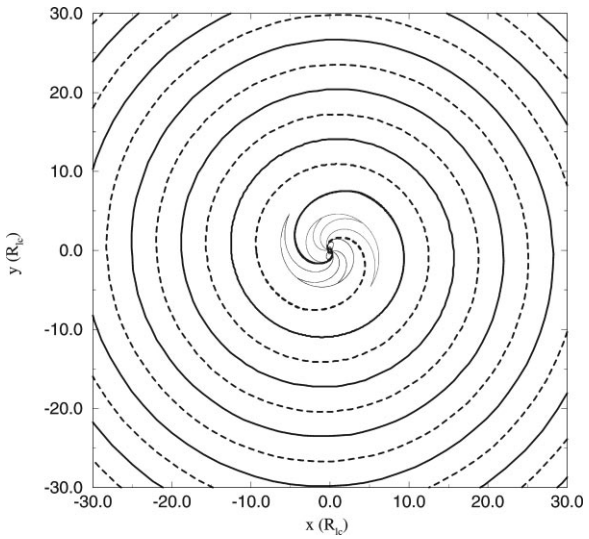

Fig. 13. Shown is the only two Archimedes spirals that are allowed by the magnetic field structure in the equatorial wave zone. Same parameters as in Fig. 12 are used.

the intense pulsar far fields has been an important topic over the years due to its possible implications for cosmic rays and the excitation of plerions [26,27]. These considerations have become even more important with the Hubble Space Telescope discovery that the pulsar in the Crab Nebula seems to have a jet coming out along what seems to be the spin axis, which is at first invisible but then excites a knot of emission very near the pulsar. At about 10 times further out the jet seems to create a shock wave, evidenced by a second knot that moves chaotically around. Beyond this apparent shock one find a very long jet visible most easily in X-rays [28]. The nature of the first knot is quite open since one would not expect a flow to shock twice. If one uses standard estimates of magnetic field strength in the Nebula, one would expect that the magnetic field at this first knot to be about 10^{-2} G. This field would not be a static field but the field of a circularly polarized wave being emitted by the rotating pulsar. There are important questions about the stability of electromagnetic waves from a pulsar [29,30] and one possibility is that there is wave to particle energy transfer at the distance of the first knot. An alternative is that there is a resonance with the gyrofrequency of the particles in a longitudinal (static) component of the magnetic field with the rotation rate of the waves. The latter consideration inspired a careful examination of such a process, which we review in increasing steps of detail. We start with the planar wave in order to understand particle's general behavior, then we discuss the particle motion in the full Deutsch fields. However, we must emphasize that the following is not intended as a review of wave-particle interactions [31], a subject that ranges over a vast landscape, but simply provides a text-book level analysis to provide a standardized starting point for electromagnetic wave emission from pulsars.

9. Pickup and acceleration in planar waves (exact)

A particularly simple case is when particles start at the axis of rotation of an orthogonal magnetic dipole. Along this axis, the radiated electromagnetic waves will be circularly polarized

and the huge intensity of such fields (in the case of pulsar modeling) should sweep up any plasma near the wave zone and drive it away from the neutron star. If we approximate the wave as a plane wave, a number of interesting phenomena appears: (1) the solutions are exact and analytic, (2) the acceleration is only temporary, and the wave cyclically reabsorbs the particle energy, (3) the critical parameter in determining a particle's energy is the ratio of wave frequency and particle cyclotron frequency, (4) resonance takes place when the frequency of the wave (ω) *equals* the particle cyclotron frequency in the steady axial field component, i.e., $\omega = \omega_{\|}$ because for particles starting from rest, $\gamma(1 - \beta_{\|}) = 1$.

9.1. Nonrelativistic case

For a circularly polarized wave moving in the $+z$ direction we will have oscillating $\boldsymbol{E}$ and $\boldsymbol{B}$ fields in both the x and y directions. Thus the Lorentz force reads

$$m\frac{\mathrm{d}v_x}{\mathrm{d}t} = e(E_x + 0 - v_z B_y)\,, \tag{99}$$

$$m\frac{\mathrm{d}v_y}{\mathrm{d}t} = e(E_y + v_z B_x - 0)\,, \tag{100}$$

$$m\frac{\mathrm{d}v_z}{\mathrm{d}t} = e(0 + v_x B_y - v_y B_x)\,. \tag{101}$$

(Later we will include a static B_z component.) Let us select the case where the fields rotate counterclockwise in the $x - y$ plane, as shown in Fig. 14 where the instantaneous $\boldsymbol{E}\times\boldsymbol{B}$ drift velocity would be in the $+z$ direction, and the test particle is an electron ($e = -e_0$). The rotating fields can be written (propagation in vacuo),

$$E_x = cB_{\perp}\cos\phi\,, \tag{102}$$

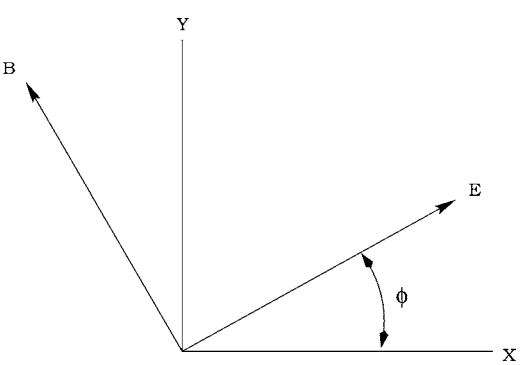

Fig. 14. The circularly polarized wave fields as seen looking in the $-z$ direction.

$$E_y = cB_\perp \sin\phi\,, \tag{103}$$

$$B_x = -B_\perp \sin\phi\,, \tag{104}$$

$$B_y = B_\perp \cos\phi\,, \tag{105}$$

with

$$\phi = \omega t - kz + \phi_0\,, \tag{106}$$

where ϕ_0 is an arbitrary phase factor, which will henceforth be set to zero.

9.2. The textbook solution

The standard analytic approach is to look for harmonic solutions. Here we have set $B_z = 0$ (we will put it back in almost immediately). The obvious solution can be gotten from inspection since the equilibrium solution will have $\boldsymbol{v}$ orthogonal to $\boldsymbol{E}$, which means that the velocity is parallel to the wave magnetic field and those components of the Lorentz force vanishes. Thus the electron will only see the electric field and will in effect act like a particle on a string being swung around at the rotational rate ω with the centrifugal force balancing the electric force (Fig. 15):

$$mv_\perp\omega = e_0 E = e_0 cB_\perp\,, \tag{107}$$

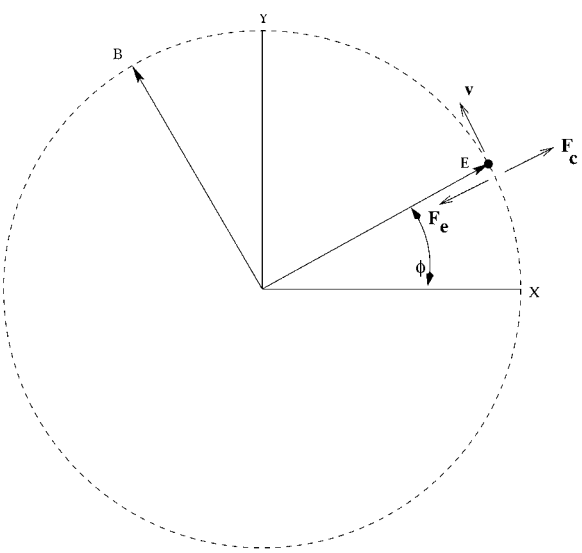

Fig. 15. Inhomogeneous solution for electron in rotating wave fields. Here the velocity is orthogonal to $\boldsymbol{E}$ such that centrifugal and electric forces balance. Consequently, $\boldsymbol{v}$ parallels $\boldsymbol{B}$ and the Lorentz forces all balance with an arbitrary velocity in the z direction. But this is not the general solution.

where e_0 is the magnitude of the electron charge (in order that we can define the cyclotron frequency as a positive quantity without negative signs) and $v_\perp$ is the circular speed,

$$v_\perp = c\frac{\omega_\perp}{\omega}, \tag{108}$$

where $\omega_\perp$ is the non-relativistic cyclotron frequency at the wave's magnetic field,

$$\omega_\perp \equiv \frac{e_0 B_\perp}{m}. \tag{109}$$

Notice immediately that one could easily have $v > c$, at low enough wave frequency in which case we would need to return and do the problem relativistically. This observation is a central consideration here. Continuing with the nonrelativistic limit for the moment, we can see that the acceleration along the z axis is zero and hence v_z can be any constant. Explicitly writing out this solution, we have

$$v_x = -v_\perp \sin\phi\,, \tag{110}$$

$$v_y = v_\perp \cos\phi\,, \tag{111}$$

$$v_z = \text{const}\,. \tag{112}$$

We can explicitly substitute these into the Lorentz equations and see that they are satisfied.

However, if we put some numbers in here we can see that this solution is preposterous! Even at the distance of the apparent shock along the spin axis of the pulsar (the second, much more distant knot), the expected wave magnetic field would be of the order of $B_\perp \approx 10^{-3}$ G or an electron cyclotron frequency of about $\omega_\perp \approx 2\times 10^4$. Since the rotational frequency of the Crab pulsar is roughly 200 rad/s, we see that the perpendicular velocity would have to be $200c$! Obviously a non-relativistic treatment is insufficient and the simplest reinterpretation is that the Lorentz factor should enter as a change in effective mass, $m \to \gamma m$ in Eq. (107), and therefore $\gamma \approx 200$. But even with this quick fix we still have a problem: where could the electron get an energy of 50 MeV simply in order to run around in a circle?

But textbooks give derivations just like the one above. What is the problem? The problem is that the answer is incomplete, it is only the *inhomogeneous* part of the solution. The inhomogeneous part is the part having *no* free parameters. Thus the particle initial condition cannot be varied. That is, of course, exactly what the homogeneous part of the solution is for. The homogeneous part is implicitly discarded at various places in many textbooks because the author is not interested in it for one reason or another (e.g., a harmonically bound electron in an electromagnetic wave to illustrate scattering, etc.). But it breeds a bad habit as illustrated here. The most likely initial condition is for a wave to overrun an electron at rest, not an electron that happens to have energy 50 MeV and moving in just the right direction.

9.3. *Particle pickup from rest* (*nonrelativistic case again*)

Now consider the case where a charged particle suddenly finds itself at rest at some phase of such a wave instead of dutifully circling. Nowhere is the particle at rest in the above solutions. But this

solution is the standard one found in standard plasma textbooks about plasma motion in a circularly polarized wave (with $v_z = 0$ in addition). It is plausible that the mean velocities might be zero *before the wave is introduced*. But the typical argument is that these velocities are somehow zero *after* the wave is introduced, which we immediately show to be incorrect.

The simple answer for the motion starting from rest is that, if we see the circular motion in a moving system with the same velocity $v_\perp$, the particle will repeatedly come to rest (at $\phi = 0$). It is immediately clear then that the x and y velocities are instead

$$v_x = -v_\perp \sin\phi\,, \tag{113}$$

$$v_y = v_\perp(\cos\phi - 1)\,. \tag{114}$$

However, now the particle has a uniform component of motion, so as it moves, it sees the alternating B_x which causes it to oscillate up and down along the z axis, since now the Lorentz force reads

$$m\frac{\mathrm{d}v_z}{\mathrm{d}t} = e(v_\perp B_x) = ev_\perp B_\perp \sin\phi \tag{115}$$

and therefore

$$v_z = v_{||}(1 - \cos\phi)\,, \tag{116}$$

where again we need a constant term if the particle started from rest (at $\phi = 0$), and

$$v_{||} = v_\perp\frac{\omega_\perp}{\omega} = c\left(\frac{\omega_\perp}{\omega}\right)^2. \tag{117}$$

Thus an electron is accelerated forward with the wave. This acceleration is rarely seen in the standard plasma physics textbook treatments because the mean velocities are all assumed to be zero *after* the wave is introduced. It is tempting to view this acceleration as being due to "radiation pressure", but as we will see, it is really a coherent wave-particle interaction since the particle will *return to rest*.

9.4. Nonlinear terms

Having uniform and harmonic components to v_z is not entirely innocuous because the term kz depends on z which hitherto was an independent variable. A constant z velocity simply changes the value of k (nonrelativistic equivalent of the Doppler shift), but a harmonic term in k makes it time dependent, and our whole treatment becomes approximate. However, the time derivative of v_x now becomes

$$\frac{\mathrm{d}v_x}{\mathrm{d}t} = \frac{\mathrm{d}\phi}{\mathrm{d}t}\frac{\mathrm{d}v_x}{\mathrm{d}\phi} = (\omega - kv_z)\frac{\mathrm{d}v_x}{\mathrm{d}\phi} \tag{118}$$

and as long as $c = \omega/k$, the potentially nonlinear term $v_z B_y$ cancels out because we now have

$$m(\omega - kv_z)\frac{\mathrm{d}v_x}{\mathrm{d}\phi} = eB_\perp(c - v_z)\cos\phi \tag{119}$$

and our harmonic solutions go through exactly as before, even when v_z itself is non-uniform as is the case for particle pickup. The z component of the Lorentz force itself becomes nonlinear, but in an integrable form;

$$m(\omega - kv_z)\frac{\mathrm{d}v_z}{\mathrm{d}\phi} = e_0 v_\perp B_\perp \sin\phi \tag{120}$$

which can immediately be integrated to give the quadratic equation

$$m\left(\omega - \frac{1}{2}kv_z\right)v_z = e_0 v_\perp B_\perp(1 - \cos\phi)\,, \tag{121}$$

where the unity is the constant of integration needed if v_z starts from rest (at $\phi = 0$). If we neglect the non-linear term, we already have seen that v_z has amplitude $v_{||}$, and if we label $\beta_{nr} = v_z/c$ the above value, the relativistic value becomes

$$\beta = 1 - \sqrt{1 - 2\beta_{\mathrm{nr}}} \approx \beta_{\mathrm{nr}} + \frac{1}{2}\beta_{\mathrm{nr}}^2 + \cdots. \tag{122}$$

It may look as if this expression becomes complex for $\beta_{nr} > 1/2$, but in the relativistic treatment, m becomes γm (sort of, we will do the relativistic treatment exactly in the following section), and it is easy to show that $2\beta/\gamma$ cannot exceed unity.

As an aside, when the equations are non-linear, we no longer have the usual classification of inhomogeneous and homogeneous solutions. The analog of the inhomogeneous solution is called the *singular* solution, and the rest are the *general* solutions. The singular solution has the same properties as the inhomogeneous solution: no degrees of freedom.

9.5. Relativistic Lorentz force

The Lorentz force gives the time derivatives of the particle momenta, which in the relativistic treatment become γmv or equivalently $mc\gamma\beta$, so we now have

$$mc\frac{\mathrm{d}(\gamma\beta_x)}{\mathrm{d}t} = e(E_x + 0 - v_z B_y)\,, \tag{123}$$

$$mc\frac{\mathrm{d}(\gamma\beta_y)}{\mathrm{d}t} = e(E_y + v_z B_x - 0)\,, \tag{124}$$

$$mc\frac{\mathrm{d}(\gamma\beta_z)}{\mathrm{d}t} = e(0 + v_x B_y - v_y B_x)\,, \tag{125}$$

and the fourth (energy) equation is

$$mc^2\frac{\mathrm{d}\gamma}{\mathrm{d}t} = e(v_xE_x + v_yE_y + 0)\,. \tag{126}$$

9.6. Covariant version

Superficially, the first three come from the Lorentz force simply by multiplying every m by γ and the fourth equation simply says that work is done on the particle at rate $\boldsymbol{v}\cdot\boldsymbol{E}$. In covariant notation, the four equations are one four-vector equation,

$$m\frac{\mathrm{d}u^\alpha}{\mathrm{d}s} = \frac{e}{c}F^{\alpha\beta}u_\beta\,, \tag{127}$$

where α and β run over the four time plus coordinate components. Repeated indices (here β) are summed over all four components. The four-velocity is

$$u^\alpha \equiv \frac{\mathrm{d}x^\alpha}{\mathrm{d}s} \rightleftharpoons \gamma(c, v_i) \rightleftharpoons \gamma(c, v_x, v_y, v_z)\,, \tag{128}$$

where we contrast the indexed vectors with their explicit components. Here i is the corresponding ordinary mathematical index running over just the three coordinates. These indices are often numbered (e.g., $0, 1, 2, 3$) for no good reason, given that ordinarily vector components are just subscripted with the obvious axis symbols x, y, z. The down-index (covariant) four-velocity just differs by a sign,

$$u_\beta = \gamma(c, -v_i)\,, \tag{129}$$

which gives the invariant (scalar) equation

$$u^\alpha u_\alpha \equiv c^2 = \gamma^2\left(c^2 - \sum_i v_i^2\right) = \gamma^2(c^2 - v^2)\,, \tag{130}$$

so as usual the Lorentz factor is

$$\gamma = \frac{1}{\sqrt{1 - v^2/c^2}}\,. \tag{131}$$

Since the ordinary velocity is

$$v_i \equiv \frac{\mathrm{d}x_i}{\mathrm{d}t}\,, \tag{132}$$

it also follows from the definition of the four-velocity, Eq. (128), that

$$\gamma = \frac{\mathrm{d}t}{\mathrm{d}s}\,. \tag{133}$$

Note that relativity does not supplant the ordinary velocity, which keeps the meaning it has always had: how fast our coordinates are crossed according to our clocks.

If $\boldsymbol{v} = 0$, $\mathrm{d}t = \mathrm{d}s$ so $\mathrm{d}s$ is the time interval for a clock moving with (say) a particle, which by definition has to be the same for all observers, hence the term "proper" time. "Proper" velocity (or four-velocity) is how fast our coordinates are crossed according to the *moving* clock and is not limited to below c, a common misconception. The electromagnetic field tensor corresponds to the electromagnetic fields seen in the local rest system, and then (again writing first time and the spatial components)

$$F^{t\alpha} = (0, -E_i) \tag{134}$$

and (ε_{ijk} being the totally antisymmetric tensor that defines the usual cross-products and curls)

$$F^{\alpha j} = \left(E_i, -c\sum_k \varepsilon_{ijk}B_k\right). \tag{135}$$

(the electric field sign changes because $F^{\alpha\beta} = -F^{\beta\alpha}$ and the sum is somewhat gratuitous given that k must simply be whichever i and j are not). For $\alpha = t$ we obtain

$$mc\frac{\mathrm{d}\gamma}{\mathrm{d}s} = \frac{e}{c}\sum_j (-E_j)(-\gamma v_j)\,, \tag{136}$$

and since

$$\frac{\mathrm{d}}{\mathrm{d}s} = \frac{\mathrm{d}t}{\mathrm{d}s}\frac{\mathrm{d}}{\mathrm{d}t} = \gamma\frac{\mathrm{d}}{\mathrm{d}t}, \tag{137}$$

one set of Lorentz factors cancel leaving (after multiplying by c)

$$mc^2\frac{\mathrm{d}\gamma}{\mathrm{d}t} = e\boldsymbol{v}\cdot\boldsymbol{E}\,. \tag{138}$$

In the same way, for $\alpha = i$ we obtain

$$m\frac{\mathrm{d}(\gamma v_i)}{\mathrm{d}s} = \frac{e}{c}(\gamma c)(E_i) + \frac{e}{c}\sum_j (-\gamma v_j)\left(-c\sum_k \varepsilon_{ijk}B_k\right) \tag{139}$$

and again one set of Lorentz factors cancel to yield

$$m\frac{\mathrm{d}(\gamma\boldsymbol{v})}{\mathrm{d}t} = e(\boldsymbol{E} + \boldsymbol{v}\times\boldsymbol{B})\,. \tag{140}$$

Note that Eq. (138) must follow from Eq. (140) simply by taking the scalar product of the latter with $\boldsymbol{v}$, which leads to the unobvious but true identity that

$$\boldsymbol{v}\cdot\mathrm{d}(\gamma\boldsymbol{v}) = \mathrm{d}(\gamma)\,. \tag{141}$$

10. Relativistic exact solutions

Returning to the issue of analytic solutions, we see that just as in the non-relativistic case, we have factors $(c - v_z)$ that cancel out and we have that

$$mc\omega \frac{\mathrm{d}(\gamma\beta_x)}{\mathrm{d}\phi} = ecB_\perp \cos\phi \,, \tag{142}$$

which has the exact solution

$$\gamma\beta_x = -g \sin\phi \,, \tag{143}$$

where we define

$$g \equiv \frac{\omega_\perp}{\omega} \tag{144}$$

since we have seen this ratio appears repeatedly. The companion component is again

$$\gamma\beta_y = g(\cos\phi - 1) \,, \tag{145}$$

for particles picked up in the wave.

The two equations for z-motion and energy conservation, Eqs. (125) and (126), are remarkable in that they are identical to one another within a factor of c. Thus we can divide the one into the other and obtain

$$\frac{\mathrm{d}(\gamma\beta_z)}{\mathrm{d}\gamma} = 1 \,, \tag{146}$$

which immediately gives, for the initial conditions (particle starting from rest) $\beta_z = 0$ and $\gamma = 1$,

$$\gamma\beta_z = \gamma - 1 \,. \tag{147}$$

This result provides an important constraint on the system. Since we have explicit expressions for all three components of momentum, we can use the identity

$$\gamma^2(\beta_x^2 + \beta_y^2 + \beta_z^2) \equiv \gamma^2 - 1 \tag{148}$$

and substitute into the left hand side of Eq. (147) gives

$$g^2(\sin^2\phi + \cos^2\phi - 2\cos\phi + 1) + (\gamma - 1)^2 = \gamma^2 - 1 \tag{149}$$

which simplifies to

$$\gamma = 1 + g^2(1 - \cos\phi) \,. \tag{150}$$

We now can solve for the z momentum obtaining

$$\gamma\beta_z = g^2(1 - \cos\phi) \,, \tag{151}$$

which are *exactly* the non-relativistic solutions. The only remaining step to finding a complete solution is to solve for $\phi(t)$, which is given from

$$\frac{\mathrm{d}\phi}{\mathrm{d}t} = \omega(1 - \beta_z) = \frac{\omega}{\gamma}\,. \tag{152}$$

Hence

$$\omega t = (1 + g^2)\phi - g^2 \sin\phi\,. \tag{153}$$

What these equations say is that the solutions are perfectly periodic but the period is increased by a factor

$$1 + g^2 \tag{154}$$

owing to the electron (or positron) "surfing" the wave, for once the particle is relativistic, the circularly polarized wave looks almost linearly polarized as the particle moves with it and is steadily accelerated.[13] Notice however that there is nothing relativistic about the solutions themselves, they are equally valid for $g \ll 1$.

We can check this result for γ (since we never used the energy term, Eq. (126), per se) by direct differentiation of Eq. (150),

$$\frac{\mathrm{d}\gamma}{\mathrm{d}t} = g^2 \sin\phi \frac{\mathrm{d}\phi}{\mathrm{d}t} = g^2 \sin\phi(\omega - k_c\beta_z) = g^2 \sin\phi \frac{\omega}{\gamma}\,, \tag{155}$$

which is indeed the energy equation multiplied by γ (one factor of g is brought in by the constant part of $\gamma\beta_y$ and ωg is just $eB_\perp/m$).

The reason we make this point is that our relativistic results are perhaps counter-intuitive. For $g \ll 1$ (non-relativistic) the larger g the higher the x and y velocities. But this behavior reverses for $g \gg 1$, where the Lorentz factor increases as g^2 but $\gamma\beta_x$ only increases as g. Thus the velocities in the x–y plane *decrease* as the particle gets accelerated to ever higher energies. Mathematically, this decrease means that the momentum in the z direction hogs all of the energy. Physically, what happens is that the magnetic fields become so strong that the particle is almost immediately curved from the initial x-direction into the z-direction. The fact that the orbits become smaller may be significant to design of laboratory acceleration of particles to large energies.

10.1. Circular vs. linear polarization

It is not necessary that the waves be perfectly circularly polarized. If we attenuate the E_x and B_y components by a factor of α, the only change is reduce the x-component of moment by the same factor,

$$\gamma\beta_x = -\alpha g \sin\phi\,, \tag{156}$$

[13] A relevant problem is the particle motion in constant, static $\boldsymbol{E}$ and $\boldsymbol{B}$ cross fields (as compared to wave field) with $E = cB$ (e.g., [32]). If starting from rest, a particle gets a tremendous boost along the direction of $\boldsymbol{E} \times \boldsymbol{B}$ whereas it obtains no momentum along $\boldsymbol{B}$ and little along $\boldsymbol{E}$. Interestingly, $1 - \beta_z = 1/\gamma$, same as in the wave case.

while the z and energy equations stay in the same fixed ratio. Thus

$$\gamma = 1 + g^2(1 - \cos\phi) + \frac{1}{2}g^2(1 - \alpha^2)\sin^2\phi\,. \tag{157}$$

Notice that, as can be seen by turning off completely one or the other components, that there is a phase dependence to the maximum energy the particle ever attains, being a maximum if the particle is picked up when the (now linear) wave has its maximum field strength, and a minimum if picked up at a null.

10.2. Resonance with a static uniform B

A classical plasma physics exercise is the effect of a resonance in the dispersion relation for a circularly polarized wave propagating along the magnetic field direction in a uniformly magnetized plasma. Rather than repeat the non-relativistic treatment, we will simply modify appropriately the relativistic treatment above by adding in a static B_z component to the Lorentz force. The x and y Lorentz forces become, after rearrangement of terms

$$\frac{\mathrm{d}(\gamma\beta_x)}{\mathrm{d}\phi}(1 - \beta_z) = -g(1 - \beta_z)\cos\phi - h\beta_y\,, \tag{158}$$

$$\frac{\mathrm{d}(\gamma\beta_y)}{\mathrm{d}\phi}(1 - \beta_z) = -g(1 - \beta_z)\sin\phi + h\beta_x\,, \tag{159}$$

where

$$h \equiv \frac{e_0 B_z}{m\omega} \equiv \frac{\omega_{||}}{\omega}\,, \tag{160}$$

and h is just the dimensionless frequency ratio analog to g. Now we see that the $(1 - \beta_z)$ terms no longer cancel out. However, the remaining two Lorentz force terms are completely unchanged and we still have the extraordinary (and general) relationship that for pickup from rest

$$1 - \beta_z = \frac{1}{\gamma}\,, \tag{161}$$

so multiplying through by γ gives

$$\frac{\mathrm{d}(\gamma\beta_x)}{\mathrm{d}\phi} = -g\cos\phi - h\gamma\beta_y\,, \tag{162}$$

$$\frac{\mathrm{d}(\gamma\beta_y)}{\mathrm{d}\phi} = -g\sin\phi + h\gamma\beta_x\,. \tag{163}$$

We see that we have a very simple driven linear coupled differential equation in just the two variables $\gamma\beta_x$ and $\gamma\beta_y$. Although h and g would seem to be on similar standings, this expectation is

not correct because we can divide out g from the equation and all that does is to rescale the two variables. Thus, we can symbolically rewrite the equations in such normalized form,

$$\frac{\mathrm{d}\xi}{\mathrm{d}\phi} = -\cos\phi - h\eta\,, \tag{164}$$

$$\frac{\mathrm{d}\eta}{\mathrm{d}\phi} = -\sin\phi + h\xi\,, \tag{165}$$

where $\xi = \gamma\beta_x/g$ and $\eta = \gamma\beta_y/g$. These equations are identical to the non-relativistic ones! It is a bit simpler to differentiate one of the equations with respect to ϕ and eliminate one of the variables, giving for example

$$\frac{\mathrm{d}^2\xi}{\mathrm{d}\phi^2} = \sin\phi - h\frac{\mathrm{d}\eta}{\mathrm{d}\phi} = (1+h)\sin\phi - h^2\xi\,. \tag{166}$$

The resonance has nothing to do with the $(1+h)\sin\phi$ term but follows from the harmonic solution being at frequency ϕ when $h=1$ in the $h^2\xi$ term. The textbook approach is as usual to look for harmonic expressions for ξ and η, giving the solutions

$$\xi = -a\sin\phi\,, \tag{167}$$

$$\eta = a\cos\phi\,, \tag{168}$$

where

$$a = \frac{1}{1-h} \tag{169}$$

and one then sees the resonance at $h=1$ corresponding to $\omega = \omega_{||}$. Although this resonance condition is the obvious solution in the non-relativistic limit, it is a bit surprising to have exactly the same solution in the relativistic case where the particles "surf" along with the wave and one would not have been surprised to find the resonance Doppler shifted by one or more Lorentz factors.

The homogeneous solutions are just those at frequency h and we have then for pickup at rest at $\phi = 0$

$$\gamma\beta_x = -\frac{g}{1-h}(\sin\phi - \sin h\phi)\,, \tag{170}$$

$$\gamma\beta_y = \frac{g}{1-h}(\cos\phi - \cos h\phi)\,, \tag{171}$$

$$\gamma\beta_z = \frac{g^2}{(1-h)^2}[1 - \cos(1-h)\phi]\,. \tag{172}$$

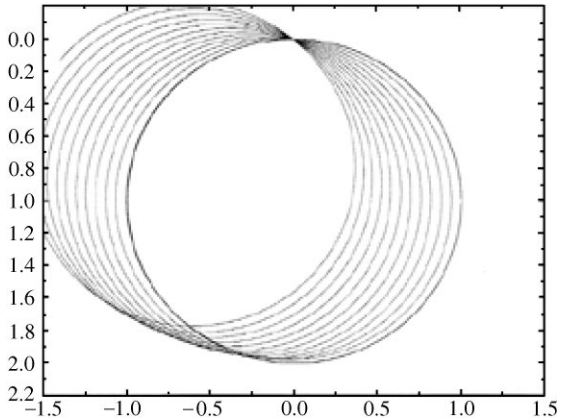

Fig. 16. Precession of the trajectory in velocity space for a non-zero longitudinal magnetic field.

The seemingly singular point at $h = 1$ does not really "blow up" the solutions because when $h \to 1$, the solutions become:

$$\gamma\beta_x = -g\phi\cos\phi\,, \tag{173}$$

$$\gamma\beta_y = -g\phi\sin\phi\,, \tag{174}$$

$$\gamma\beta_z = \frac{1}{2}g^2\phi^2\,. \tag{175}$$

These Cartesian solutions somewhat obscure what the particle is doing in velocity space, which is to execute a circle for $h = 0$ but the starting point ($\xi = \eta = 0$) is not at the center of the circle but is a point on the circle (obvious in retrospect), and for small h the circle precesses about this point, as shown in Fig. 16.

10.3. Motion in space

The progress of the particle along z can easily be gotten because

$$\frac{\mathrm{d}z}{\mathrm{d}t} = \frac{\mathrm{d}z}{\mathrm{d}\phi}\,\frac{\mathrm{d}\phi}{\mathrm{d}t} = \frac{\mathrm{d}z}{\mathrm{d}\phi}\,\omega(1-\beta_z) = \frac{\mathrm{d}z}{\mathrm{d}\phi}\,\frac{\omega}{\gamma} \tag{176}$$

but we also have that

$$\beta_z = 1 - \frac{1}{\gamma} \tag{177}$$

so all together

$$\frac{\omega}{c}\,\frac{\mathrm{d}z}{\mathrm{d}\phi} = \gamma - 1\,. \tag{178}$$

However, it is easy to see that substituting arbitrary values for η and ξ into the Lorentz identity, Eq. (148) gives

$$\gamma = 1 + \frac{1}{2}[(\gamma\beta_x)^2 + (\gamma\beta_y)^2] = 1 + \frac{g^2}{2}(\xi^2 + \eta^2) \tag{179}$$

so we find that

$$z = \frac{c}{\omega}\frac{g^2}{2}\int(\xi^2 + \eta^2)\,\mathrm{d}\phi\,, \tag{180}$$

which, for $h = 0$, has the solution,

$$z = \frac{c}{\omega}g^2(\phi - \sin\phi)\,. \tag{181}$$

Even though we opened our analysis with a discussion directed at electrons, the key conclusions (cf. Eqs. (179) and (180)) only depend on g^2, which is the same for electrons and positrons. Likewise, solutions can be generalized to protons by simply replacing m_e with the proton rest mass, and we see immediately that protons or other ions would be accelerated to much lower energies.

10.4. Particle not starting at rest

If a particle starts with a non-zero β_{z0} but $\beta_{x_o} = \beta_{y_o} = 0$, we define $\gamma(1 - \beta_z) = \gamma_0(1 - \beta_{z_o}) = c_0$, or $\beta_{z_o} = (1 - c_0^2)/(1 + c_0^2)$ and $\gamma_0 = (1 + c_0^2)/2c_0^2$, one gets

$$\gamma\beta_x = -\frac{g}{1 - h'}(\sin\phi - \sin h'\phi)\,, \tag{182}$$

$$\gamma\beta_y = \frac{g}{1 - h'}(\cos\phi - \cos h'\phi)\,, \tag{183}$$

$$\gamma\beta_z = \frac{g^2}{(1 - h')^2}\frac{1}{c_0}[1 - \cos(1 - h')\phi] + \gamma_0\beta_{z_o}\,, \tag{184}$$

$$\gamma(1 - \beta_z) = c_0\,, \tag{185}$$

where $h' = h/c_0$.

Alternatively, if $\beta_{z_o} = 0$ but $\beta_{x_o} = \beta_{y_o} \neq 0$, we define $\gamma_0 = c_0$. Then $\gamma\beta_{x_o} = \sqrt{(c_0^2 - 1)/2} = d_0$. The solutions are (again, $h' = h/c_0$):

$$\gamma\beta_x = d_0[\cos(h'\phi) - \sin(h'\phi)] + \frac{g}{1 - h'}[\sin(h'\phi) - \sin\phi]\,, \tag{186}$$

$$\gamma\beta_y = d_0[\cos(h'\phi) + \sin(h'\phi)] - \frac{g}{1 - h'}[\cos(h'\phi) - \cos\phi]\,, \tag{187}$$

$$\gamma\beta_z = \frac{g}{c_0(h'-1)}\left(d_0 + \frac{g}{h'-1}\right)[1-\cos(h'-1)\phi] - \frac{gd_0}{c_0(h'-1)}\sin(h'-1)\phi\,, \tag{188}$$

$$\gamma(1-\beta_z) = c_0\,. \tag{189}$$

In both cases, the resonant condition changes from $h = 1$ to $h/c_0 = 1$, which is obvious from the requirement $\omega - kv_z = \omega_{||}/\gamma$.

10.5. Plasma dispersion effects

An additionally curious feature of these equations that the reader may have noticed is that we have assumed that $\omega = ck$ at a number of places in the discussion. If we had a number of particles picked up in place of a single one, the natural expectation would be that the coherent conduction currents from these particles would modify the phase velocity of the wave, just as in the case of an ordinary non-relativistic plasma. In every case, the *same* ratio ω/k replaces c in every step of the derivation, so the same results obtain even for a plasma dispersed wave. For our discussion of particle motion in intense fields, the linear assumption implicit in even discussing a dispersion relation becomes inapplicable. However, for other applications this observation may be of some use.

11. Motion in realistic fields

Having discussed the particle motion in constant wave fields, we move on to more complicated situations.

11.1. Decreasing wave amplitude (*still planar*)

Given that we can solve for z as the phase ϕ advances (e.g., Eq. (180)), we can ask what happens when the wave fields E and B (parameterized as g) and radial B field (h) vary with distance, as would be the case for spherical waves instead of plane waves. To our knowledge, this second step of complication cannot be done analytically. However, since the underlying equations of motion become linear when we take the phase to be the independent variable, we have the advantage that numerical solutions of linear equations mimic the exact solutions. Thus a harmonic oscillator solved numerically (with appropriately small steps) gives exactly harmonic solutions, the only difference being that the oscillation frequency is slightly different from the continuum case (the difference vanishes as the step size vanishes). The important point then is that there is no true "error" in the numerical solution insofar as *generic* behavior goes. Consequently, introducing additional (non-linear) terms does not introduce *additional* errors but rather is the only step that introduces potential errors so long as we are basically interested in the generic behavior of systems and do not require a precision simulation of a specific system.

Neglecting first h, it is easy to show that the effect of reducing g, the wave amplitude, with distance causes the persistent y component of velocity to approach a constant fixed value which is

slightly more than half its maximum value (if one instead models the variation in terms of a monotonic dependence on ϕ rather than z, the approach turns out to be more symmetrical toward exactly 1/2). Fig. 17 shows this process. What is happening physically is that the wave having become weaker is no longer able to bring the particle back to rest and ultimately the wave becomes an irrelevant perturbation with all three components of momentum approaching fixed values. The physics is somewhat different if h, the magnetic field component parallel to the propagation direction, is non-zero, because the persistent component of velocity now circles in the B_z field as shown previously in Fig. 16. The effect of precession in a declining wave field is illustrated in Fig. 18. Thus one has a trade-off depending on which is the faster, the decline in g or the precession induced by h. If the former dominates, the system will approach nonzero values as just discussed, but if the latter dominates the system will approach zero energy!

It is straightforward to solve the set of equations (e.g., Eqs. (162), (163), (179)) numerically by introducing

$$g = g_0\left(\frac{z_0}{z}\right), \tag{190}$$

$$h = h_0\left(\frac{z_0}{z}\right)^2, \tag{191}$$

as would be the simplest behavior expected for the decline with distance from a pulsar for a wave field and a frozen-in radial component of magnetic field, respectively, with z being the distance along the spin axis. Using parameters believed to be appropriate for the Crab pulsar, we have

$$g_{\mathrm{wz}} = \frac{e_0 B_0}{m\Omega}\left(\frac{a}{R_{\mathrm{wz}}}\right)^3 = 9.5\times 10^{10} \tag{192}$$

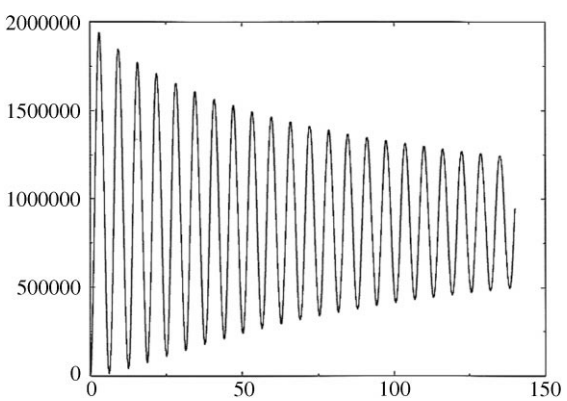

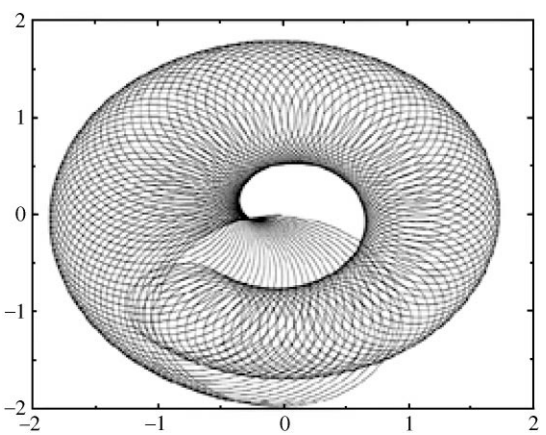

Fig. 17. Lorentz factor of a particle moving in a plane wave whose strength declines along the particle trajectory.

Fig. 18. Precession in velocity space of a particle in a declining wave field moving parallel to a static magnetic field.

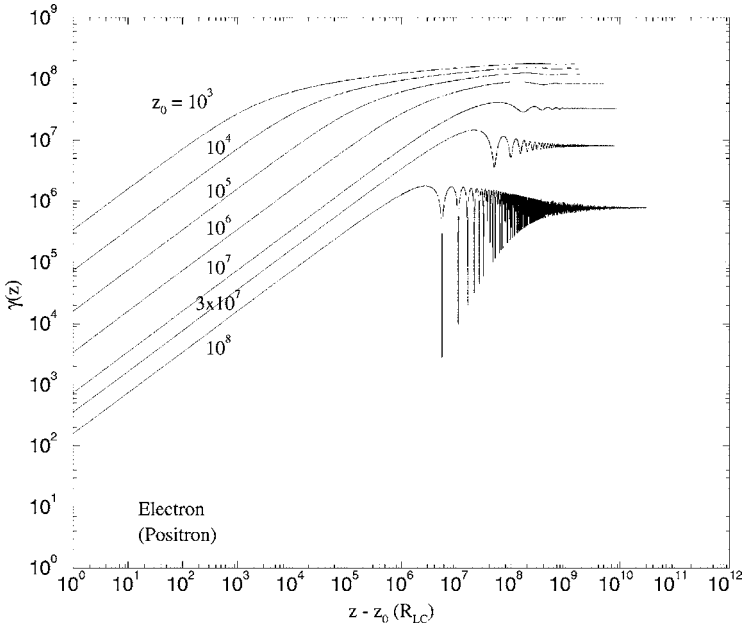

Fig. 19. Electron (or positron) energy development as a function of distance $z - z_0$ (starting from rest at various initial distances z_0) accelerated in a plane wave whose amplitude decreases as $1/z$. Parameters appropriate for Crab pulsar are used. The asymptotic energy and the pivoting distance beyond which electron shows large oscillations in energy are all in good agreement with the analytic estimates. The initial enormous energy gain comes from the fact that particles are picked up by and are almost in phase with the wave. The first decrease in energy marks the first time when a particle is out of phase with the wave.

at the wave zone distance (sometimes called the "light-cylinder" distance[14]) $R_{\rm wz} = c/\Omega$ (hereafter, all distances are in units of $R_{\rm wz}$).

Fig. 19 shows the acceleration of electrons (or positrons) starting with different initial g or effectively, different distances from the pulsar along the rotation axis. The parameter h is chosen to be zero in all these runs. The overall trend is clear that the further away a particle starts, the lower its final energy is. There also seems to be a "pivoting" behavior in electron's energy development in that the further away a particle starts, the larger the "oscillations" in its energy as a function of distance. (Such behavior is more clearly seen in the spherical wave cases considered in the following sections.) To qualitatively understand Fig. 19, recall that when previously g is a constant (and $h = 0$), the particle's energy is a periodic function of z with period $2\pi g^2$. In other words, a particle starting from rest reaches its maximum energy when $\Delta z = \pi g^2$. Now that g decreases as $1/z$, we can define a critical distance $z_{\rm c}$ by equating

$$z_{\rm c} = \pi(g_{\rm wz}/z_{\rm c})^2 \quad \text{or} \quad z_{\rm c} = (\pi g_{\rm wz}^2)^{1/3} \approx 3\times10^7. \tag{193}$$

[14] The term comes from earlier models discussed above that assumed centrifugal forces, not electromagnetic forces, were dominant in pulsar activity. In that view, we could technically still be inside the "light-cylinder" if on the spin axis.

Thus, we are faced with two possibilities of either $z_0 < z_c$ or $z_0 > z_c$, which are equivalent to $z_0 < \Delta z$ and $z_0 > \Delta z$, respectively. The pivoting behavior can be understood as follows: Particles starting inside the critical distance z_c will be continuously accelerated until they reach beyond z_c where particle starts to become out of phase with the wave *and* the strength of the wave has decreased enough. That the actual "turning points" in Fig. 19 are larger than z_c can be understood as overshooting since particles already have enormous energies as they advance each decade in z. Particles starting beyond z_c, on the other hand, will reach their highest energy when $\Delta z = z - z_0 \approx \pi(g_{wz}/z_0)^2$. For example, at roughly the distance to knot 2 (the possible shock) for the Crab, we have $z_0 = 10^8$, and $\Delta z \sim 3 \times 10^6 \ll z_0$, so $g(z)$ is effectively the same as $g(z_0)$.

The maximum energy a particle can obtain in such fields can be estimated again from the constant g case (which is $2g^2$). Similarly,

$$\gamma_{max} \approx 2\left(\frac{g_{wz}}{z_c}\right)^2 \approx 2 \times 10^7, \quad z_0 < z_c\,, \tag{194}$$

$$\gamma_{max} \approx 2\left(\frac{g_{wz}}{z_0}\right)^2, \quad z_0 > z_c\,. \tag{195}$$

The actual final energies shown in Fig. 19 are higher than the above estimate when $z_0 < z_c$ due to the continuous acceleration between z_0 and z_c. For $z_0 > z_c$, the above equation gives a good agreement. Lower particle energies also enable waves to "take back" most of the particle energy as the particle moves in and out of phase with the wave, as evidenced by the large amplitude oscillations in $\gamma(z)$.

11.2. $h \neq 0$ case

By letting $h_{wz} = g_{wz}$ at the wave zone distance, we can explore the effects due to a nonzero B_z. Since $h \sim 1/z^2$, the condition for $h = 1$ will occur at $z \sim 3 \times 10^5$. On the other hand, the particle dynamics is still controlled by staying in phase with the wave due to the large wave amplitude (i.e., $g \sim 1/z$), the Lorentz force due to $p_{x,y}B_z$ is comparatively insignificant until the particle starts to slip out of phase with the wave. By that time, the distance is so large ($z \geq z_c$) that wave becomes so weak that it could not strongly affect particle motion anymore. When starting at $z = 10^4$, Fig. 20 shows that there is essentially no difference in electron energy gain with $h \neq 0$. Fig. 21 compares the electron and positron energy gain with $h \neq 0$. Again, only little difference is seen.

Although the resonance does not play a role in the particle's dynamics, if a particle is starting very close to the wave zone, the B_z component will become important. A distance can be roughly estimated by balancing the two Lorentz force components, $g_{wz}/z \sim p_{x,y}g_{wz}/z^2$, which gives $z \sim p_{x,y}$. So, during the acceleration phase, if $p_{x,y}$ exceeds z, the particle will experience gyration around B_z, thus limiting the magnitude of the transverse momentum. Consequently, the particle final energy is reduced also.

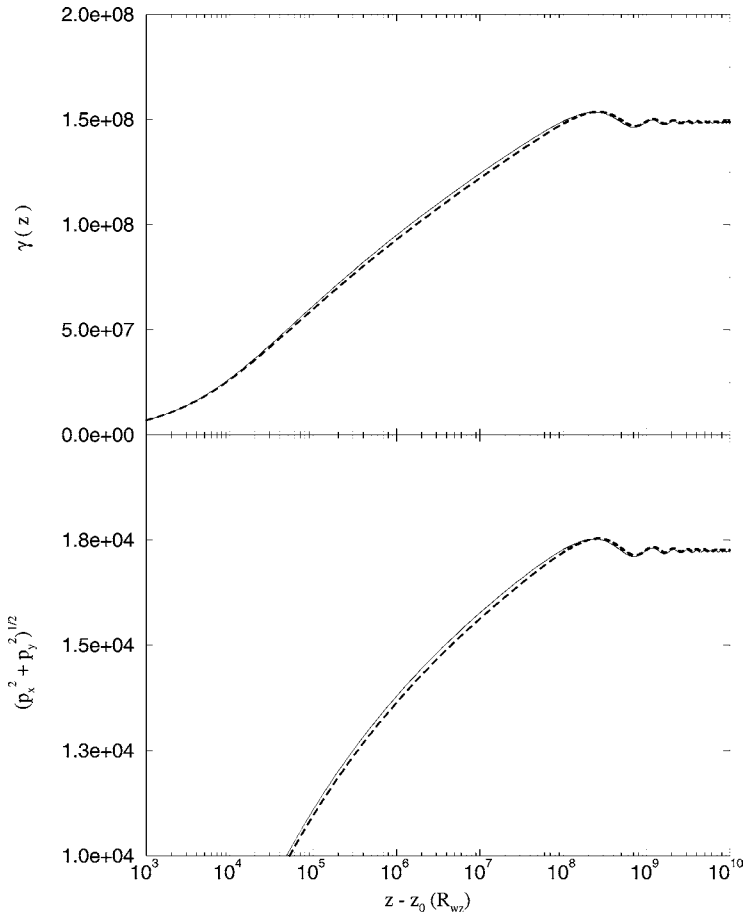

Fig. 20. Upper panel shows the energy development of an electron accelerated in a planar wave as a function of distance $z - z_0$ starting from rest at $z_0 = 10^4$. Lower panel shows the corresponding evolution of the transverse momentum. Parameters appropriate for Crab pulsar are used. The solid and dashed curves are for $h = 0$ and $h = g_{wz}/z^2$, respectively. It is clear that there is hardly any difference between these two cases.

11.3. Motion in spherical waves

The true fields from a rotating pulsar will be spherical instead of planar at large distances. As we will show, there is a subtle but important first order error if the spherical wave is treated as simply a plane wave whose strength drops appropriately with distance (i.e., the discussion in the proceeding section).

For an orthogonal rotator ($\sin\xi = 1$), the pure spherical vacuum wave along the rotation axis ($\cos\theta = 1$) can be expressed as

$$B_r = E_r = 0\,, \tag{196}$$

$$B_\theta = -E_\phi/c = B_{wz}\cos\psi\,\frac{1}{R}\,, \tag{197}$$

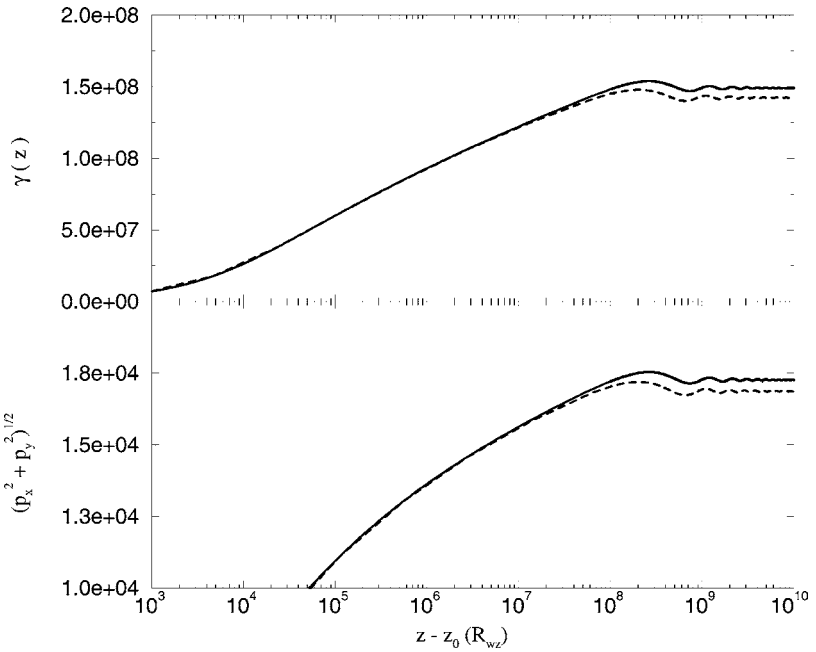

Fig. 21. Upper panel shows the electron and positron energy development accelerated in a planar wave as a function of distance $z - z_0$ starting from rest at $z_0 = 10^4$. Lower panel indicates the changes in the transverse momentum. Parameters appropriate for Crab pulsar are used. The solid and dashed curves are for electron and positron, respectively. Again, $h = g_{wz}/z^2$. There is only very little difference between electrons and positrons due to a non-zero h.

$$B_\phi = E_\theta/c = -B_{wz}\sin\psi\frac{1}{R}, \tag{198}$$

where $R = r/R_{wz}$ is the dimensionless radial distance, $B_{wz} = B_0(a/R_{wz})^3$ is the B field at R_{wz}, $\psi = \phi + R - \Omega t = \phi - \phi_s$, and $\phi_s = \Omega t - R$. For the sake of completeness, we write out the Lorentz equation of a charged particle q in spherical coordinates by taking the dot product of $\hat{e}_r$, $\hat{e}_\theta$, and $\hat{e}_\phi$ with $\mathrm{d}\boldsymbol{p}/\mathrm{d}t = q(\boldsymbol{E} + \boldsymbol{v}\times\boldsymbol{B})$, since it proves fruitful to think of the particle motion in $\{r, \theta, \phi\}$ rather than $\{x, y, z\}$ as in the planar case. Substituting the above expressions for field components, we can write the three components plus energy equation as (see also [33]).

$$\frac{\mathrm{d}p_r}{\mathrm{d}s} = \frac{p_\theta^2 + p_\phi^2}{R} - g_{wz}\frac{q}{|q|}\frac{1}{R}(p_\theta\sin\psi + p_\phi\cos\theta\cos\psi), \tag{199}$$

$$\frac{\mathrm{d}p_\theta}{\mathrm{d}s} = \frac{p_\phi^2\cot\theta - p_r p_\theta}{R} - g_{wz}\frac{q}{|q|}\frac{1}{R}(\gamma - p_r)\sin\psi, \tag{200}$$

$$\frac{\mathrm{d}p_\phi}{\mathrm{d}s} = -\frac{p_\theta p_\phi\cot\theta + p_r p_\phi}{R} - g_{wz}\frac{q}{|q|}\frac{1}{R}(\gamma - p_r)\cos\theta\cos\psi, \tag{201}$$

$$\frac{\mathrm{d}\gamma}{\mathrm{d}s} = -g_{\mathrm{wz}}\frac{q}{|q|}\frac{1}{R}(p_\theta \sin\psi + p_\phi \cos\theta\cos\psi)\,, \tag{202}$$

$$\frac{\mathrm{d}w}{\mathrm{d}s} \equiv \frac{\mathrm{d}(\gamma - p_r)}{\mathrm{d}s} = -\frac{p_\theta^2 + p_\phi^2}{R}\,, \tag{203}$$

where we define here the dimensionless proper time interval $\mathrm{d}s = \Omega\,\mathrm{d}t/\gamma$, the dimensionless momentum components $p_r = \gamma\beta_r = \mathrm{d}R/\mathrm{d}s, p_\theta = \gamma\beta_\theta = R\,\mathrm{d}\theta/\mathrm{d}s$, and $p_\phi = \gamma\beta_\phi = R\sin\theta\,\mathrm{d}\phi/\mathrm{d}s$. A new variable $w = \gamma - p_r$ is used to indicate whether a particle hogs most of its energy in radial component or whether it is gaining energy in the transverse components. The first terms on the right-hand side are geometric terms due to the fact that $\hat{e}_i \cdot \mathrm{d}\hat{e}_j/\mathrm{d}t$ is usually not zero, or they can be thought of as inertial terms (e.g., centrifugal and Coriolis forces) in the non-Cartesian coordinate system.

It is tempting to solve the equations directly in spherical rather than Cartesian coordinates, which is indeed convenient for particles starting with large θ, say, from the equator. But for particles starting along the rotation axis ($\theta = 0$), there is an awkward singularity ($\cot\theta$) in the θ and ϕ momentum equations, which complicates numerical calculations. One way to get around is to solve the Cartesian equations when θ is very small but switch to spherical coordinates otherwise.[15] Ostriker and Gunn [2] considered the special case with particles starting at the equator ($\theta = \pi/2$), effectively removing this singularity.

This set of Lorentz equation proves to be harder to solve than its counterpart in the planar wave case, mainly due to the fact that one has to track the phase term $\psi = \phi - \phi_{\mathrm{s}}$ very carefully since it is a function of both time and position. The time derivative of a quantity X can be expressed as $\mathrm{d}X/\mathrm{d}s = (\mathrm{d}X/\mathrm{d}\phi_{\mathrm{s}})(\mathrm{d}\phi_{\mathrm{s}}/\mathrm{d}s)$ and $\mathrm{d}\phi_{\mathrm{s}}/\mathrm{d}s = \gamma(1-\beta_r)$. In the planar wave case, ϕ is not defined (thus is a constant effectively), and $\gamma(1-\beta_z) \equiv 1$, which allows a great simplification by transferring time derivatives into phase derivatives. As shown in Eq. (203), $\gamma(1-\beta_r)$ is *not* a constant in the spherical wave. In fact, as we will show below, $\gamma(1-\beta_r)$ varies from 1 to $\sim 1/\gamma$.

On the other hand, Ostriker and Gunn [2] argued that the phase ϕ_{s} does not change appreciably for particles close to the light-cylinder and with this important simplification, they were able to obtain some analytic solutions for a test particle picked up by a plane-polarized spherical wave from the equatorial plane ($\theta = \pi/2$). Here, by rigorously tracking the phase and solving the full set of equations, we are able to confirm the key assumption used in [2] and explore parameter regimes when this assumption is not applicable. For example, when particles start at large distances, they experience large variations in the angle ϕ. Another example is when the full Deutsch fields are used, which will be discussed in the next section. An additional motivation for accurate motion determination is the consequent implications for calculating its radiation in the pulsar fields.

Fig. 22 shows the particle energy in a spherical wave as a function of R starting with different heights on the spin axis z_0. Again, we see a "pivoting" behavior in the particle energy development depending on whether $z_0 < z_{\mathrm{c}}$ or not, where z_{c} is the same as Eq. (193). Particles starting within z_{c} are continuously accelerated without any decrease in energy whereas particles starting with $z_0 > z_{\mathrm{c}}$ show large energy "oscillations", and the run with $z_0 = z_{\mathrm{c}} \approx 4\times 10^7$ indicates the transition between these two types of motion.

[15] The codes used to solve the equation of motion in this and following sections can be obtained by contacting Hui Li at hli@lanl.gov.

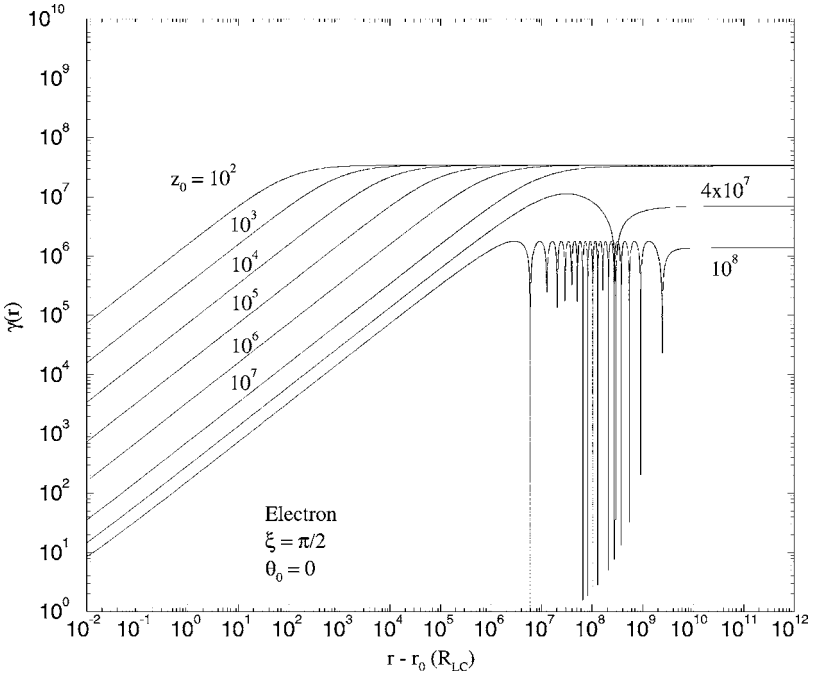

Fig. 22. Electron (or positron) energy development as a function of distance $r - r_0$ accelerated in a spherical wave whose amplitude decreases as $1/r$. Parameters appropriate for Crab pulsar are used with $\xi = \pi/2$ and particles are placed at rest on the rotation axis with various initial heights z_0. All length scales are in units of $R_{wz} \approx 1.5 \times 10^8$ cm. For $z_0 < z_c = 3 \times 10^7$, particles reach maximum energy in $\sim 2r_0$ and no energy decrease is seen because particles have not yet been overtaken by another cycle of the wave. Note the differences when compared with the plane wave case (Fig. 19).

In order to better understand the results in Fig. 22, we can describe the initial motion of an electron in a pure spherical wave by first considering a tiny increase in $\phi_s = \Omega t - R$ from $0 \to \varepsilon$. This makes $\psi \to -\varepsilon$ which implies $E_\phi \approx -1$ and $E_\theta \approx 0$. Thus the angle ϕ changes from $0 \to \pi/2$ as soon as electron moves away from the axis, which then makes $\psi \approx \pi/2 - \varepsilon$. Consequently, $\sin\psi \approx 1$ and $\cos\psi \approx 0$. The equation of motion of an electron can then be further simplified (making use the fact that $p_\phi \ll p_r, p_\theta$) as

$$\frac{\mathrm{d}p_r}{\mathrm{d}s} \approx \frac{p_\theta^2 + g_{wz} p_\theta}{R}, \tag{204}$$

$$\frac{\mathrm{d}p_\theta}{\mathrm{d}s} \approx \frac{-p_r p_\theta + g_{wz} w}{R}, \tag{205}$$

$$\frac{\mathrm{d}\gamma}{\mathrm{d}s} \approx \frac{g_{wz} p_\theta}{R}, \tag{206}$$

$$\frac{\mathrm{d}w}{\mathrm{d}s} \approx -\frac{p_\theta^2}{R}. \tag{207}$$

Armed with these simple equations, we note the following features of particle motion in a pure spherical wave:

First, the physics for this strong particle acceleration follows because particles stay more in phase with the wave. Note that even though the wave is circularly polarized along the spin axis, elliptically polarized at some intermediate θ angle and plane polarized at the spin equator, a particle picked up from rest essentially sees a plane polarized wave (e.g., $E_\theta \approx -1$ and $E_\phi \approx 0$ in the above example). So the analysis by [2] applies here. Eq. (207) shows that $\gamma(1-\beta_r)$ is driven from 1 at $t=0$ to $\ll 1$ at later time, giving

$$\beta_r \to 1 - \frac{1}{2\gamma^2}\,, \tag{208}$$

or equivalently, β_θ, $\beta_\phi \to 0$. Notice that the equivalent expression for a plane wave is

$$\beta_z = 1 - \frac{1}{\gamma}\,. \tag{209}$$

When using parameters typical of the Crab pulsar nebula, the extra power of γ at large values of this parameter makes a huge difference in the asymptotic behavior, with the effect that a particle (even though it is moving at less than the speed of light), will for all practical purposes never be overtaken by another cycle of the wave, i.e., it will be at such huge distances that interaction with the local interstellar medium will become dominant. For example, in order for ϕ_s to increase by π, Ωt has to be $\sim 2\pi\gamma^2$, which would require a distance of ~ 100 kpc (!) if $\gamma \sim 10^7$. This behavior is not what one would get for a plane wave whose strength is made to drop, because there the particle ends up with a non-zero transverse momentum, and the proper velocity parallel to the (plane) wavefront does not represent the proper velocity parallel to the curved wavefront, which is asymptotic to the total proper velocity of the particle, as illustrated in Fig. 23. Treating the wave as plane gives us instead Eq. (209) so that particle is constrained in z propagation and slips out of phase with the wave at $\Omega t \sim \pi\gamma$.

Second, the total amount of energy a particle can get depends on the transverse momentum p_θ and p_ϕ. This is not surprising since an electron has to move parallel to the electric field to gain energy. Above equations indicate that for particles starting from rest, p_θ will increase first, so will

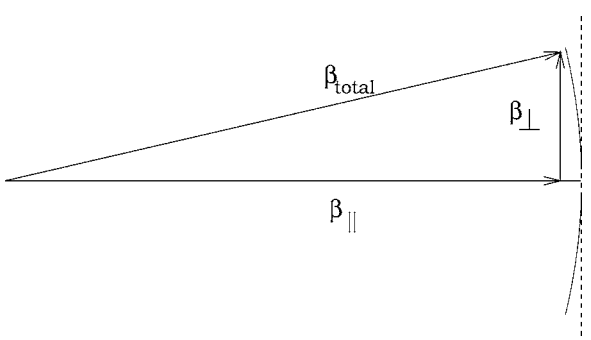

Fig. 23. Edge-on view of plane and spherical wave showing that the velocity vector is significantly closer to the spherical wave when there is a velocity component parallel to the wave front.

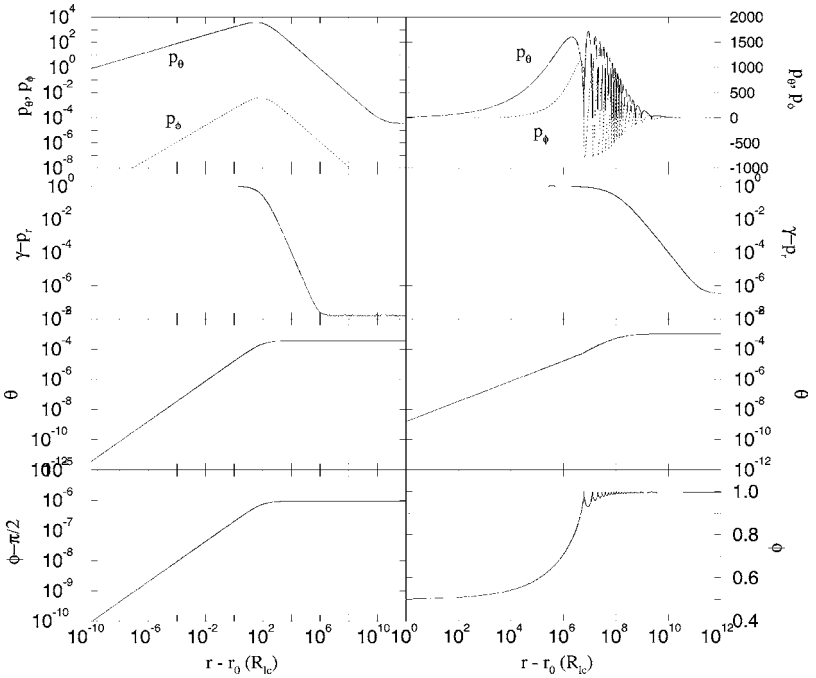

Fig. 24. The details of an electron's energy development and position changes for $z_0 = 100$ (left panel) and $z_0 = 10^8$ (right panel) respectively. Notice the different scales for these two cases. All other parameters are the same as in Fig. 22. Note that electron reaches its maximum energy when p_θ is the largest. Also, $\gamma - p_r = \gamma(1 - \beta_r) \approx 1/(2\gamma_\infty) \sim 10^{-8}$ and $\sim 3 \times 10^{-7}$, respectively.

γ and p_r ($w \approx 1$). The continuous growth of γ depends on p_θ being positive. But Eq. (205) implies that p_θ will reach a maximum when $g_{\rm wz} w = p_r p_\theta$, from which point p_θ starts to decrease. The decrease of p_θ will eventually diminish the increase of γ and the decrease of w implies that essentially all the particle's momentum is in $\hat{e}_r$ direction. Consequently, particle starts "coasting" in energy with p_θ, p_ϕ, and w all asymptotically being zero.

Fig. 24 shows in greater detail the evolution of several key quantities with $z_0 = 100$ (left panel) and $z_0 = 10^8$ (knot 2 distance in Crab nebula, right panel). One can see that for $z_0 = 100$, p_θ stays positive so particle energy γ never decreases. This is not true for $z_0 = 10^8$, in which case the wave is much weaker, a particle, even though still gains quite an amount of energy, repeatedly goes out of phase with the wave (note also the oscillations in p_θ and p_ϕ) and consequently will be brought to rest and be reaccelerated, until the particle has gone far enough that the wave is too weak to bring particle completely to rest. In both cases, the main particle motion in real space is straight up along the spin axis. For $z_0 < z_{\rm c}$, there is a tiny translation away from the rotation axis with no "circulation" since ϕ stays essentially constant. Whereas for $z_0 > z_{\rm c}$, there is a rotation about the axis that is translated away from the spin axis (due to positive p_θ).

Third, particles obtain the same asymptotic energy as long as $z_0 < z_{\rm c}$ and they reach that energy at $R \sim 2z_0$. This is quite different from the planar wave case (i.e., comparing Figs. 19 and 22). To

estimate the asymptotic particle energy in spherical wave, we can take the ratio of Eqs. (206) and (205),

$$\frac{\mathrm{d}\gamma}{\mathrm{d}p_\theta} \approx \frac{g_{\mathrm{wz}} p_\theta}{g_{\mathrm{wz}} w - p_r p_\theta} \tag{210}$$

which at early time ($w \approx 1$ and $p_r p_\theta \ll g_{\mathrm{wz}}$) gives $\gamma \approx p_\theta^2$. On the other hand, p_θ will reach its maximum when $g_{\mathrm{wz}} w = p_r p_\theta$, which implies $p_\theta \approx g_{\mathrm{wz}}/\gamma$. Equating $\gamma \approx p_\theta^2$ and $p_\theta \approx g_{\mathrm{wz}}/\gamma$, we get

$$\gamma \approx g_{\mathrm{wz}}^{2/3} \approx 2 \times 10^7 \tag{211}$$

which is in good agreement with Fig. 22. Note that this dependence is quite different from the planar wave case in Eq. (194). In estimating the final energy, there is no distance scale involved (as long as $z_0 < z_c$). We can roughly estimate the distance where $\gamma_{\max}$ is reached by noting that $\mathrm{d}s = \Omega \mathrm{d}t/\gamma \approx \mathrm{d}R/\gamma$. Substituting this into Eq. (206), we get

$$\frac{\mathrm{d}R}{R} \approx \frac{\mathrm{d}\gamma^{3/2}}{g_{\mathrm{wz}}} \Rightarrow \Delta R \approx R\,. \tag{212}$$

This is again in agreement with Fig. 22. Note that γ_∞ in spherical wave is smaller than the planar waves because particle motion is slightly more limited in transverse directions, whereas transverse motion/displacement is necessary for particle to gain energy from the E field. This difference is evident by comparing the amplitude of transverse momentum in Figs. 20 and 24.

The results given in Eq. (211) also agree with those in [2], where $\gamma \propto g_{\mathrm{wz}}^{2/3}(1 - R_0/R)^{2/3}$. When $\Delta R = R - R_0 \ll R_0$, this indicates that γ increases as $\Delta R^{2/3}$, which is in perfect agreement with Fig. 22.

For $z_0 > z_c$, the final particle energy is determined by $\sim 2(g_{\mathrm{wz}}/z_0)^2$, which is the same as in the planar wave case (cf. Eq. (195)) for the same physical reason. This again agrees with Fig. 22.

11.4. Motion in Deutsch fields

The Deutsch fields at $R \gg R_{\mathrm{wz}}$ are given in Section 7 but are recaped here,

$$B_r \approx 2B_{\mathrm{wz}} \frac{1}{R^2} \sin\xi \sin\theta \sin\psi\,,$$

$$E_r \approx B_{\mathrm{wz}} \frac{c}{R^2} \frac{2}{3} \cos\xi\,,$$

$$B_\theta \approx -E_\phi/c \approx B_{\mathrm{wz}} \frac{1}{R} \sin\xi \cos\theta \cos\psi\,,$$

$$B_\phi \approx E_\theta/c \approx -B_{\mathrm{wz}} \frac{1}{R} \sin\xi \sin\psi\,. \tag{213}$$

It is straightforward to write down the equation of motion of a charged particle q in Deutsch fields (without radiation reaction). Define $\boldsymbol{B}'/R = \boldsymbol{B}/B_{\rm wz}$ and $\boldsymbol{E}'/R = \boldsymbol{E}/(cB_{\rm wz})$, it reads

$$\frac{\mathrm{d}p_r}{\mathrm{d}s} = \frac{p_\theta^2 + p_\phi^2}{R} + g_{\rm wz}\frac{q}{|q|}\frac{1}{R}(\gamma E'_r + p_\theta B'_\phi - p_\phi B'_\theta)\,, \tag{214}$$

$$\frac{\mathrm{d}p_\theta}{\mathrm{d}s} = \frac{p_\phi^2\cot\theta - p_r p_\theta}{R} + g_{\rm wz}\frac{q}{|q|}\frac{1}{R}(\gamma E'_\theta + p_\phi B'_r - p_r B'_\phi)\,, \tag{215}$$

$$\frac{\mathrm{d}p_\phi}{\mathrm{d}s} = -\frac{p_\theta p_\phi\cot\theta + p_r p_\phi}{R} + g_{\rm wz}\frac{q}{|q|}\frac{1}{R}(\gamma E'_\phi + p_r B'_\theta - p_\theta B'_r)\,, \tag{216}$$

$$\frac{\mathrm{d}\gamma}{\mathrm{d}s} = g_{\rm wz}\frac{q}{|q|}\frac{1}{R}(p_r E'_r + p_\theta E'_\theta + p_\phi E'_\phi)\,, \tag{217}$$

$$\frac{\mathrm{d}w}{\mathrm{d}s} = -\frac{p_\theta^2 + p_\phi^2}{R} + g_{\rm wz}\frac{q}{|q|}\frac{1}{R}(-wE'_r + p_\theta(E'_\theta - B'_\phi) + p_\phi(E'_\phi + B'_\theta))\,. \tag{218}$$

The Deutsch fields are asymptotically pure spherical vacuum waves for sufficiently large R, so only when particles start close to $R_{\rm wz}$ are there significant differences. So one would expect the same particle behavior as described in spherical wave case when R is sufficiently large (we will quantify this statement soon).

We again consider an orthogonal rotator ($\sin\xi = 1$) with an electron starting on the spin axis. Fig. 25 shows particle's energy development in Deutsch fields. Again, the physics for particle acceleration is unchanged compared to the pure spherical wave case. And indeed, particle's behavior is the same as in a spherical wave when $z_0 > 10^4$.

Comparing with the pure spherical wave (cf. Fig. 22), Fig. 25, however, depicts marked difference when $z_0 \le 10^4$ (the change is obviously continuous). To understand this difference, we again follow the arguments in deriving Eqs. (204)–(207) where $\psi = \pi/2 \pm \varepsilon$. We obtain

$$\frac{\mathrm{d}p_r}{\mathrm{d}s} \approx \frac{p_\theta^2 + g_{\rm wz}p_\theta}{R}\,, \tag{219}$$

$$\frac{\mathrm{d}p_\theta}{\mathrm{d}s} \approx \frac{-p_r p_\theta + g_{\rm wz}w}{R}\,, \tag{220}$$

$$\frac{\mathrm{d}\gamma}{\mathrm{d}s} \approx \frac{g_{\rm wz}p_\theta}{R}\,, \tag{221}$$

$$\frac{\mathrm{d}w}{\mathrm{d}s} \approx -\frac{p_\theta^2}{R} + \frac{g_{\rm wz}p_\theta}{R}(B'_\phi - E'_\theta)\,, \tag{222}$$

which are the same as Eqs. (204)–(207) except the last equation on $\mathrm{d}w/\mathrm{d}s$ where we keep an extra term. Using the expressions given in Section 7, it can be rigorously shown that $B'_\phi - E'_\theta \approx \sin\psi/R^2 \approx 1/R^2$, *different from spherical wave* where $B'_\phi - E'_\theta \equiv 0$. Even though this difference is

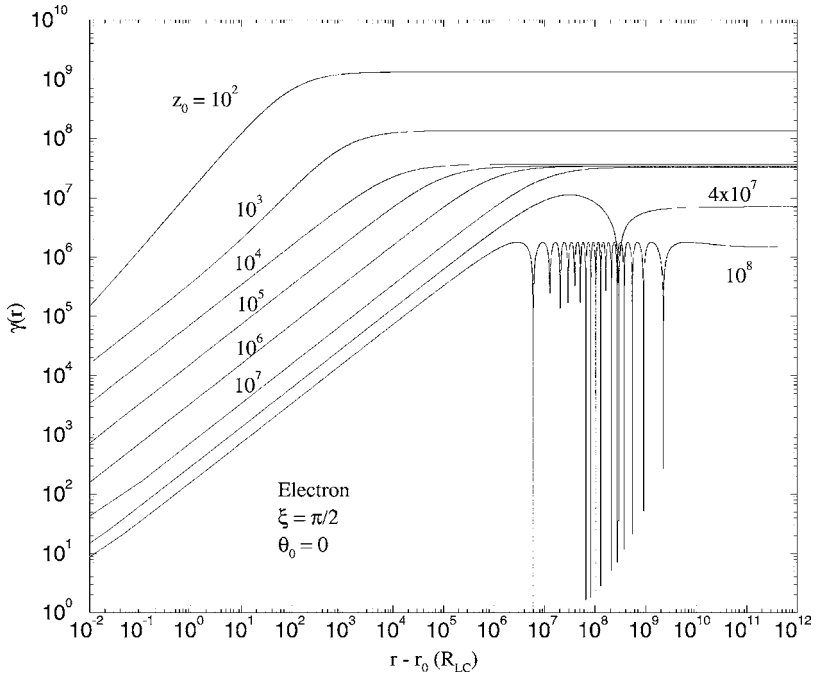

Fig. 25. Similar to Fig. 22 but in Deutsch field of an orthogonal rotator instead of a pure spherical wave. Particles are more strongly accelerated in a Deutsch field when starting relatively close by ($z_0 \leq 10^3$).

much smaller than the *strength* of the field itself ($1/R$ vs. $1/R^2$), it constitutes an important contribution in Eq. (222) because g_{wz}/R^2 can still be much larger than p_θ. This seemingly "small" difference is *solely* responsible for the large increase in γ when $z_0 \leq 10^4$ in Fig. 25. We now discuss why this is the case.

Eq. (222) guarantees that $w = \gamma - p_r$ should *increase* initially since $g_{wz}/R^2 > p_\theta$. This is contrary to the spherical wave case where w is *always* decreasing. Physically it means that not all the energy is going into the radial momentum, and the increase in w makes the maximum p_θ even larger. As discussed before, the larger the p_θ, the higher the γ. As both p_θ and R increase, it comes to a point when $g_{wz}/R^2 = p_\theta$ (or $dw/ds = 0$) which implies $R \approx (g_{wz}/p_\theta)^{1/2} \approx 10^4$ if $p_\theta \sim 10^3$. This is consistent with Fig. 25 in which the run of $z_0 = 10^4$ already shows a slightly higher final γ. Eventually, w starts to decrease and becomes much less than one (i.e., radial component hogs all the energy), particle starts to coasting with the wave with no transverse momentum. Fig. 26 compares the different behavior for an electron in Deutsch fields and spherical wave with the same initial $z_0 = 100$. It confirms the above analytic estimates.

11.5. Role of a non-zero B_r

The effect of a non-zero B_r is unimportant in the cases we considered here because particles are picked up at the rotation axis (i.e., $\sin\theta \approx \theta \ll 1$). This, however, is not the case if a particle starts at the equatorial plane of the rotation axis.

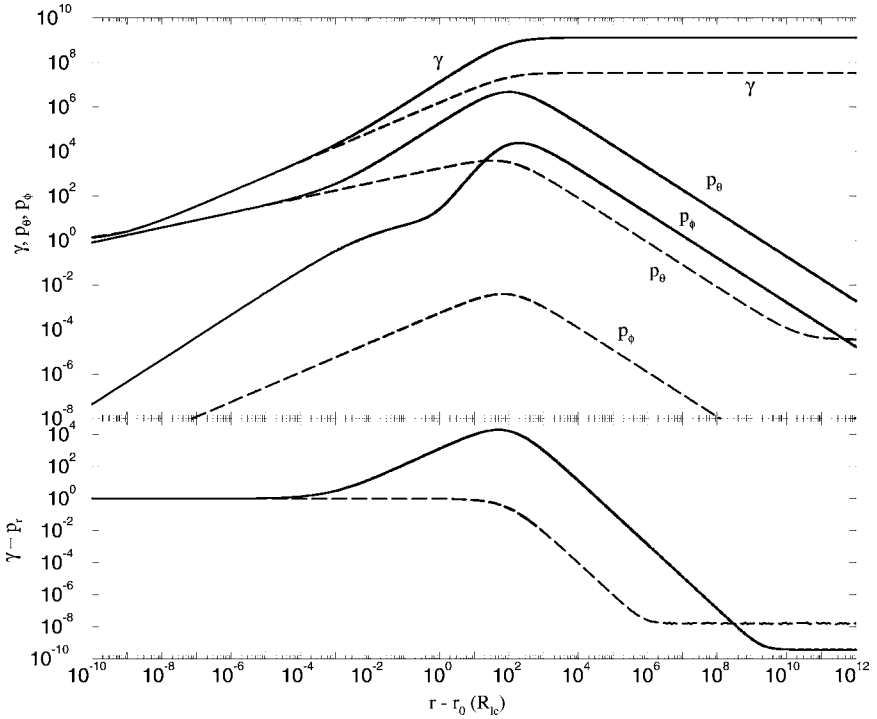

Fig. 26. A detailed comparison of an electron's energy development (starting at $z_0 = 100$) in a Deutsch field (solid lines) and a pure spherical wave (dashed lines). The fact that $\gamma - p_r$ can be much larger than 1 results in a much larger p_θ, thus rendering higher asymptotic particle energy in the Deutsch field.

In the planar wave case, we have discussed the effect of a nonzero B_z by pointing out the possibility of resonance via $\gamma(1-\beta_z) = (eB_z/m)/\Omega$, or, $h = eB_z/m\Omega = 1$ because $\gamma(1-\beta_z)$ is always 1. We also showed that this resonance does not really influence the dynamics of particle motion. In the spherical wave (or Deutsch field) case, there is an equivalent resonant condition due to a non-zero B_r,

$$\gamma(1-\beta_r) = \frac{eB_r}{m\Omega}. \tag{223}$$

We can see that the resonant condition changes from $h = 1$ in the planar wave case to $h = \gamma(1-\beta_r) \approx 1/2\gamma \ll 1$ for spherical waves. Using $\gamma \sim 2\times 10^7$, this requires an exceedingly small B_r ($\sim 3\times 10^{-13}$ G when $\Omega \approx 200$ rad/s), which is impractical. Physically, it means that a particle is moving *along* B_r so close to the speed of light, the wave frequency seen by the particle is very small.

The actual B_r will always be much larger than the required B_r given above for resonance to occur. Though B_r does not influence the particle dynamics via resonance, it could potentially have a strong effect on a particle motion by forcing the particle into gyration if p_θ and p_ϕ are large enough. Imagine instead of B_r decreases continuously as $1/r^2$, it approaches a constant after some finite distance, then depending on the strength of B_r and the magnitude of transverse momentum, it will reduce the particle final energy by limiting the maximum transverse momentum. For this effect

to occur, the Lorentz force components due to $p_\theta B_r$ and $p_\phi B_r$ have to be important *during the acceleration phase*. Otherwise, during the "coasting" stage, even if B_r is comparable to B_θ and B_ϕ, it will not make any difference because p_θ and p_ϕ are essential zero.

11.6. Ions, positrons vs. electrons

For an orthogonal rotator, the energy development of electrons and positrons is essentially indistinguishable when $z_0 > 100$. For an inclined rotator ($\xi \neq \pi/2$), the electric dipole field E_r due to the central charge ($2/3 \cos \xi$) cannot be completely ignored even when launching particles in the wave zone. One tends to think that the presence of a positive E_r helps (hinders) positrons (electrons) gaining energy. But the gained energy is in the *radial* component, which hinders (helps) positrons (electrons) gaining transverse momentum. So, these two effects tend to cancel each other, and the net difference in final energy between an electron and a positron is less than 10% when $z_0 = 100$ (not shown here). This dipole field, however, could be important for particles injected *at* the wave zone.

We have also studied the proton motion in the same Deutsch field and Fig. 27 indicates that they follow basically the same behavior as electrons except to reduce $g_{\rm wz}$ by m_p/m_e. Thus, protons asymptotically reach a Lorentz factor of $\sim 10^5$ (i.e., $\sim 10^{14}$ eV) versus $\gamma \sim 2 \times 10^7$ (i.e., $\sim 10^{13}$ eV) for electrons. This is very different from parallel electric field acceleration where electrons and ions are expected to gain the same energies on average.

Another effect which is not discussed here is that the electron motion in real space is different from that of positron, even though they gain the same energy (probably at the same rate). This

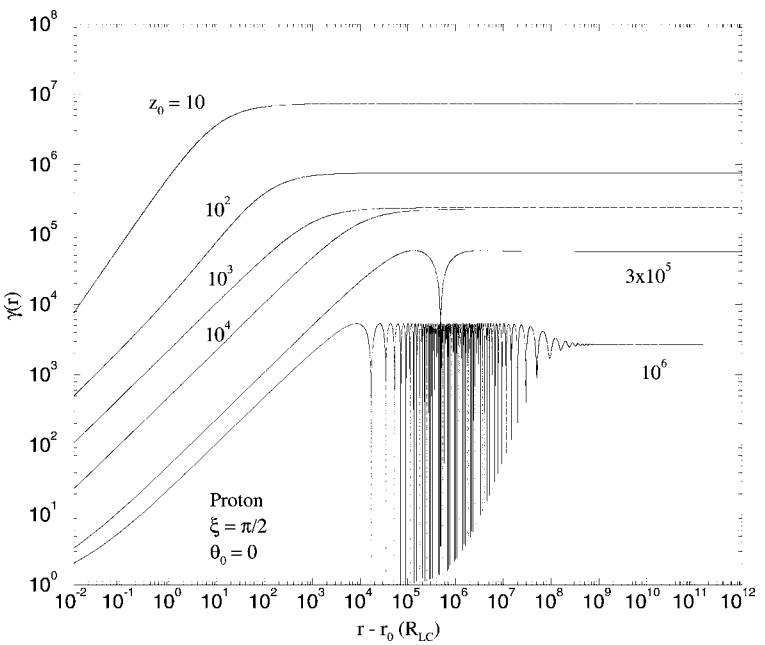

Fig. 27. Similar to Fig. 25 but for protons. The asymptotic energy is approximately reduced by a factor of $(m_{\rm p}/m_{\rm e})^{2/3}$.

might produce charge separation in space between electrons and positrons as they are accelerated away.

11.7. Plasma dispersion effects

So far, we have been studying the dynamics of a test particle injected into the wave zone of a vacuum wave field ($E = cB$) from an inclined magnetic rotator. Thus, the generic picture is that strong waves "drag" particles with themselves and accelerate them to extremely high energies. Obviously when enough particles are injected into this field, wave energy will likely be absorbed by particles and instead one has a relativistic MHD flow (see the next section). Ostriker and Gunn [2] pointed out that vacuum-like propagation of the wave requires the wave frequency to exceed the effective plasma frequency, which implies an upper limit of the particle injection rate into the wave zone, above which MHD theory should apply. Arons [34] further discussed this point and argued that most pulsar theories predicted higher particle injection rates. Another argument that has been discussed in literature is that even if the particle injection rate is low enough so that the wave frequency is still above the plasma frequency, the wave will have a phase speed $E/B > c$. Since the basic mechanism discussed in previous sections relies so critically on the "phase-locking" between the particle and the wave, even a little plasma will "destroy" this matching. Here, we want to show that particles actually are accelerated even more strongly when the wave has $E/B > c$, contrary to the common conception.

We will follow the approach in Ref. [2] since it is analytically much simpler and tractable. Near the equatorial plane of the rotation, we modify the plane-polarized spherical wave as the following:

$$B_r = E_r = 0\,, \tag{224}$$

$$B_\theta = E_\phi = 0\,, \tag{225}$$

$$B_\phi = -B_{\rm wz}\sin\psi\frac{1}{R}\,, \tag{226}$$

$$\frac{E_\theta}{c} = -fB_{\rm wz}\sin\psi\,\frac{1}{R}\,, \tag{227}$$

where we have introduced a factor $f(\geq 1)$ to mimic the effects of plasma dispersion causing $E/B > c$. The simplified Lorentz force on an electron is then

$$\frac{{\rm d}p_r}{{\rm d}s} \approx \frac{p_\theta^2}{R} + \frac{g_{\rm wz}}{R}p_\theta\,, \tag{228}$$

$$\frac{{\rm d}p_\theta}{{\rm d}s} = \frac{-p_r p_\theta}{R} + \frac{g_{\rm wz}}{R}(f\gamma - p_r)\,, \tag{229}$$

$$\frac{{\rm d}\gamma}{{\rm d}s} = \frac{g_{\rm wz}}{R}fp_\theta\,, \tag{230}$$

$$\frac{{\rm d}w}{{\rm d}s} \equiv \frac{{\rm d}(\gamma - p_r)}{{\rm d}s} = -\frac{p_\theta^2}{R} + (f-1)\frac{g_{\rm wz}}{R}p_\theta\,. \tag{231}$$

Note the additional positive $(f-1)$ term in $\mathrm{d}w/\mathrm{d}s$. This is very similar to the Deutsch field case (cf. Eq. (222)) where $w=\gamma-p_r$ is shown to *increase* first (cf. Fig. 26). Physically, the larger E (or $f>1$) ensures that a larger transverse momentum p_θ will be reached, hence the particle's final energy will increase. Carrying out the detailed derivations, one finds that

$$p_\theta \approx (2w\gamma + (f^2-1)\gamma^2)^{1/2}\,, \tag{232}$$

where the first term on the right-hand-side is the original Ostriker and Gunn solution. If we approximate $f=1+\varepsilon$ with $\varepsilon \ll 1$, then we have two possibilities. One is that $w=\gamma-p_r>\varepsilon\gamma$ or $\varepsilon<1-p_r/\gamma$ for *all* γ, then the perturbation f on the wave is so small that it gives essentially the same results as if $E/B=c$. On the other hand, if $\varepsilon>1-p_r/\gamma$, then the rate of increase of p_θ can be much higher. Consequently, we get

$$\gamma \approx \sqrt{2\varepsilon} f^2 g_{\mathrm{wz}} \ln(R/R_0)\,, \tag{233}$$

which can be compared to the result from [2]

$$\gamma \approx g_{\mathrm{wz}}^{2/3}(1-R_0/R)^{2/3}\,. \tag{234}$$

Note the different power dependence on g_{wz}.

Let's use the Crab pulsar as an example. We will assume $\varepsilon=10^{-5}$. As a particle is accelerated from rest, the initial behavior should be the same as in a pure vacuum wave until $\varepsilon\gamma\sim 1$, after which p_θ is dominated by the $(f^2-1)\gamma^2$ term in Eq. (232). So, there will be an enhanced acceleration after $\gamma>1/\varepsilon\sim 10^5$. Furthermore, during this enhanced acceleration, particle's γ should increase as $\Delta R=R-R_0$ as predicted by Eq. (233). This is different from Eq. (234) where γ increases as $\Delta R^{2/3}$. Eq. (234) also implies that acceleration essentially stops when, say, $R=2R_0$, where Eq. (233) will predict a continuing acceleration for $R\gg R_0$, though it gradually levels off also. All these features are confirmed in Fig. 28.

Since $g_{\mathrm{wz}}\sim 10^{11}$ for Crab pulsar, we can also estimate a critical $\varepsilon\approx 5\times 10^{-8}$, above which the final energy reached in a wave with $E/B>c$ can be substantially higher than that in a pure vacuum wave $E/B=c$.

11.8. Comparison with MHD wind solutions

In the MHD relativistic wind models from pulsars, a critical parameter is the dimensionless ratio of the Poynting flux in the magnetized wind to the rest mass energy flux carried by the particles, or

$$\sigma=\frac{B^2}{\mu_0 fmc^2}\,, \tag{235}$$

where f is the number flux of particles cross a sphere of radius r as counted in the rest system. Since $B\approx 1/r$, the value of σ is independent of radius and is therefore a constant of the motion for the flow. If one can estimate the particle injection rate and magnetic field at some known distance, one can estimate σ [35]. Furthermore, one can infer from σ what the asymptotic Lorentz factor of the flow might be, the usual estimate being [35]

$$\gamma \approx \sigma^{1/3}\,. \tag{236}$$

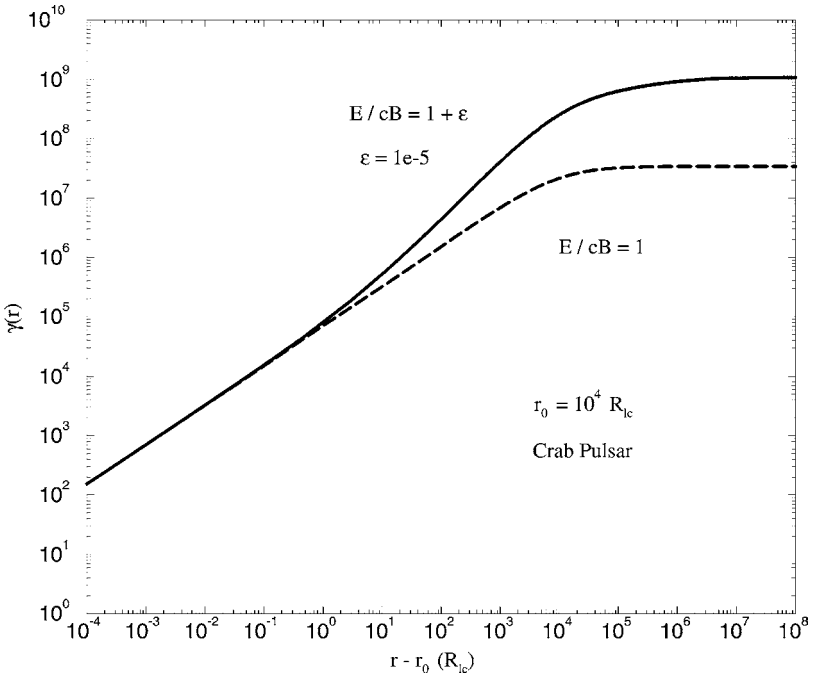

Fig. 28. A comparison between the electron acceleration in a pure vacuum wave ($E/B = c$) and a wave mediated by some plasma ($E/B > c$). Parameters similar to Crab pulsar are used.

Kennel and Coroniti [36] have applied such models to the Crab pulsar, but have chosen to use a different definition (which we designate $\sigma*$),

$$\sigma* \equiv \frac{\sigma}{\gamma}. \tag{237}$$

Here the dimensionless ratio $\sigma*$ measures the relative energy flux in the fields versus the particles. The motivation seems to come from the idea that observation might more easily constrain $\sigma*$ (which in turn determines the power input from the pulsar to the nebula) than σ (which requires an estimate of both B and the injection rate). However, from a theoretical point of view σ signifies a boundary condition for the flow while $\sigma*$ specifies a *solution* that results from this boundary condition. As a result, considerable confusion has been propagated in follow-on papers: if a paper specifies σ, the goal is likely to be to calculate in effect the asymptotic Lorentz factor, while if a paper specifies $\sigma*$, it is assuming that the relative power outputs are known, and the goal may or may not to be to see if that number can be theoretically justified.

For the Crab pulsar parameters, both the MHD and the particle pickup estimates are similar, $\gamma \approx 10^7$, but we have to regard this similarity to be something of a coincidence. For a single particle introduced into a vacuum electromagnetic wave from a vacuum rotator, both σ and $\sigma*$ would be infinite. Indeed, we could turn the problem around and calculate what particle flux could be

tolerated before the wave energy was largely transfered to the particles. Then in a sense we would be looking for solutions with $\sigma* \approx 1$. Such wave-particle calculations are of high interest, but given that the phase-locking is such a delicate but important issue even in the vacuum case, and given that particle loading will perturb the wave phase as part of the loading mechanism, all the present calculations can serve for is as a template for future many particle or MHD-like calculations.

11.9. Radiation reaction and quantum corrections

Since particles are accelerated to extremely high energies ($\gamma \sim 10^7$–10^8) and the magnetic field is reasonably strong, it is natural to ask whether particle energy gain process is balanced by radiation damping long before the particle gets these extreme energies. Shen [37] presented a thorough discussion of these issues and the validity of classical electrodynamics with possible quantum corrections.

The radiation reaction of relativistic particles depends on the magnitude and direction of acceleration, regardless of the specific cause of acceleration. If particles *always* start from rest, Shen [37] has argued convincingly that the radiation reaction (damping) effect is almost negligible. The main reason for this is that the radiative damping force depends on both the particle's energy and the angle between the particle's motion and the field. The particle tends to align itself to have minimum perpendicular acceleration. This is *not* the case when the particle enters the fields with a large Lorentz factor.

However, the issue of single-particle radiation reaction is something of a red herring given that sufficient particle fluxes should be leaving an active pulsar to act like a plasma and the coherent radiation reaction on a plasma is generally huge compared to Thomson scattering off the individual particles. Since the quasi-linear plasma theory is not even close to being valid for the large amplitude waves from pulsars, entirely new approximations will have to be developed.

12. Conclusions

Our intention for Part I (Sections 1–7) is to provide a standard set of background fields as starting points for pulsar theoretical modeling. It is not an intention to be dictatorial in the sense that these fields *must* be used, but rather again to establish a standard for comparison. If an author wishes for whatever reason to omit yet again the central charge on an aligned rotator, so be it but please at least explicitly admit it and not leave it to the reader to puzzle through the results before suddenly realizing that omission.

Insofar as Part II (Sections 8–11) goes, here again we hope to at least establish the minimal consequences of plasma from the pulsar being injected into the fields of Part I. Even there we have been able to do little more than scratch the surface. Issues remain unresolved such as how the non neutral plasma is arrayed about an inclined rotator, how to best model pair production, where transitions from corotation in the inner magnetosphere to wave pickup in the outer magnetosphere takes place, and ultimately, what do any of these models have to do with the radio pulsars that they are expected to simulate.

Acknowledgements

Useful discussions with Jon Weisheit and Stirling Colgate are gratefully acknowledged. FCM thanks the support of a grant from NASA, NAG-5-3070, and HL's research is supported by an Oppenheimer Fellowship at LANL.

References

[1] A.J. Deutsch, Ann. d'Astrophysique 18 (1955) 1.
[2] J.P. Ostriker, J.E. Gunn, Ap. J. 157 (1969) 1395.
[3] A. Hewish, S.J. Bell, J.D.M. Pilkington, P.F. Scott, R.A. Collins, Nature 217 (1968) 709.
[4] F.C. Michel, Theory of Neutron Star Magnetospheres, University of Chicago Press, Chicago, 1991.
[5] W.K.H. Panofsky, M. Phillips, Classical Electricity and Magnetism, Addison-Wesley, Reading, MA, 1955, 344 pp.
[6] F.C. Michel, Rev. Mod. Phys. 54 (1982) 1.
[7] J. Krause-Polstorff, F.C. Michel, MNRAS 213 (1985) 43.
[8] L.D. Landau, E.M. Lifshitz, Electrodynamics of Continuous Media, Reed Edu. and Prof. Ltd, 1984, 220 pp.
[9] L.I. Schiff, Proc. Natl. Acad. Sci. 25 (1939) 391.
[10] R.A.R. Tricker, Contributions of Faraday and Maxwell to Electrical Science, Pergamon Press, Oxford, 1966, 31 pp.
[11] R.N. Manchester, J.H. Taylor, Pulsars, Freeman, San Francisco, 1977.
[12] J.H. Malmberg, J.S. deGrassie, Phys. Rev. Lett. 35 (1975) 577.
[13] L.R. Brewer, J.D. Prestage, J.J. Bollinger, W.M. Itano, D.J. Larson, D.J. Wineland, Phys. Rev. A 38 (1988) 859.
[14] J.J. Heinzen, J.J. Bollinger, F.L. Moore, W.M. Itano, D.J. Wineland, Phys. Rev. Lett. 66 (1991) 2080.
[15] P. Goldreich, W.H. Julian, Astrophys. J. 157 (1969) 869.
[16] L. Mestel, M.H.L. Pryce, Mon. Not. R. Astron. Soc. 254 (1992) 355.
[17] A. Musmilov, A.K. Harding, Astrophys. J. 485 (1997) 735.
[18] V.S. Beskin, A.V. Gurevisch, I.N. Istomen, Astrophys. Space Sci. 146 (1988) 205.
[19] T. Erber, Rev. Mod. Phys. 38 (1966) 626.
[20] P.D. Thacker, MS Thesis, Rice University, 1998.
[21] N.J. Holloway, Nature (Phys. Sci.) 246 (1973) 6.
[22] P.D. Thacker, F.C. Michel, I.A. Smith, Revista Mexicana de Astronomia y Astrofisica Serie de Conferenias, 1997.
[23] J.L. Parish, Astrophys. J. 193 (1974) 225.
[24] J.H. Cohen, A. Rosenblum, Astrophys. Space Sci. 16 (1972) 130.
[25] K.O. Thielheim, H. Wolfsteller, Astrophys. J. (Suppl.) 71 (1989) 583.
[26] J.E. Gunn, J.P. Ostriker, Astrophys. J. 165 (1971) 523.
[27] C.F. Kennel, R. Pellat, J. Plasma Phys. 15 (1976) 335.
[28] J.J. Hester et al., Astrophys. J. 448 (1995) 240.
[29] F.V. Coroniti, Astrophys. J. 349 (1990) 538.
[30] F.C. Michel, Astrophys. J. 431 (1994) 397.
[31] H. Karimabadi, K. Akimoto, N. Omidi, C.R. Menyuk, Phys. Fluids B 2 (1990) 606.
[32] L.D. Landau, E.M. Lifshitz, The Classical Theory of Fields, Butterworth-Heinemann, London, 1975, 58 pp.
[33] K.O. Thielheim, Astrophys. J. 409 (1993) 333.
[34] J. Arons, in: G. Setti, G. Spada, A. W. Wolfendale (Eds.), Origins of Cosmic Rays, Reidel, Dordrecht, 1981, 175 pp.
[35] F.C. Michel, Astrophys. J. 158 (1969) 727.
[36] C.F. Kennel, F.V. Coroniti, Astrophys. J. 283 (1984) 694.
[37] C.S. Shen, Phys. Rev. D 17 (1978) 434.